ŞEHİR VE BÖLGE PLANLAMA ALANINDA AKADEMİK TARTIŞMALAR

Editör: Doç.Dr. Fuat BAŞÇİFTÇİ

yaz
yayınları

Şehir ve Bölge Planlama Alanında Akademik Tartışmalar

Editör

Doç.Dr. Fuat BAŞÇİFTÇİ

yaz yayınları

2026

yaz
yayınları

Şehir ve Bölge Planlama Alanında Akademik Tartışmalar

Editör: Doç.Dr. Fuat BAŞÇİFTÇİ

E_ISBN 978-625-8996-63-0

Haziran 2026 – Afyonkarahisar

Dizgi/Mizanpaj: YAZ Yayınları

Kapak Tasarım: YAZ Yayınları

YAZ Yayınları. Yayıncı Sertifika No: 73086

M.İhtisas OSB Mah. 4A Cad. No:3/3
İscehisar/AFYONKARAHİSAR

www.yazyayinlari.com

yazyayinlari@gmail.com

İÇİNDEKİLER

AN INTEGRATED FRAMEWORK FOR URBAN GROWTH MODELLING IN TRANSPORTATION CORRIDORS USING REMOTE SENSING, GIS, AND LOGISTIC REGRESSION[1]

Gülsüm Ecem DEMİRDAĞ[2]

Kemal Mert ÇUBUKÇU[3]

1. INTRODUCTION

Urbanization is widely recognized as one of the most transformative processes shaping contemporary landscapes. Beyond the concentration of population in urban areas, urbanization represents a multidimensional process of spatial transformation that restructures land-use systems and alters the relationships between natural, agricultural, and built environments. Since the second half of the twentieth century, rapid urban expansion has become a dominant feature of global development, with built-up areas growing at rates that often exceed population growth. As a result, urban areas have expanded beyond their traditional boundaries, exerting increasing pressure on surrounding rural landscapes, agricultural land, and natural ecosystems (Antrop 2004; Seto, Güneralp, and Hutyra 2012).

---

[1] This chapter is derived from the doctoral dissertation entitled Spatial Analysis of the Effects of Highway Investments on Agricultural Lands, completed by the author in 2026 at the Graduate School of Natural and Applied Sciences, Dokuz Eylül University.

[2] Research Assistant Dr., Department of City and Regional Planning, Faculty of Architecture, Mersin University, Mersin, Türkiye, ORCID: 0000-0001-6876-2114.

[3] Prof. Dr., Department of City and Regional Planning, Faculty of Architecture, Dokuz Eylül University, İzmir, Türkiye, ORCID: 0000-0003-3604-7014.

In recent decades, these processes have increasingly been discussed within the context of land take, which refers to the conversion of agricultural, forest, and other natural or semi-natural lands into artificial surfaces. Land take is associated not only with the physical expansion of urban areas but also with the loss of ecosystem services, landscape fragmentation, and declining agricultural functions (EEA 2006; ESPON 2020). Consequently, understanding the mechanisms that drive land-use change has become a central concern in spatial planning and land management studies.

Among the factors influencing urban growth, transportation infrastructure plays a particularly important role. Improvements in accessibility alter development opportunities, affect land values, and influence the spatial distribution of investment and population. Previous studies have demonstrated that highways frequently stimulate urban expansion by encouraging residential, commercial, and industrial development in previously less accessible locations (Baum-Snow 2007; Duranton and Turner 2012; Kasraian et al. 2016). These effects are especially visible around highway interchanges, where accessibility advantages often generate concentrated development pressures and accelerate land-use conversion processes (Chi 2010; Garcia-López 2012; Müller, Steinmeier, and Küchler 2010).

The consequences of transportation-induced urban growth are particularly significant for agricultural land. Numerous studies have shown that urban expansion often occurs at the expense of productive agricultural areas, resulting in farmland loss, fragmentation, and reduced landscape continuity (Lambin and Meyfroidt 2011; Turner et al. 2020; Wu 2019). Understanding where these transformations occur, how they evolve over time, and which factors drive them is therefore essential for sustainable spatial planning.

Advances in remote sensing and Geographic Information Systems (GIS) have considerably improved the ability to monitor and analyse long-term land-use dynamics. Multi-temporal satellite imagery provides consistent observations of land-use change, while spatial modelling approaches facilitate the investigation of the factors influencing these changes and support the development of future land-use scenarios (Lu and Weng 2007; Veldkamp and Lambin 2001; Wulder et al. 2019).

This chapter presents an integrated framework for analysing urban growth processes in transportation corridors through the combined use of remote sensing, GIS, multi-criteria evaluation, and logistic regression modelling. The framework is demonstrated using the İzmir–Denizli Motorway corridor in western Türkiye, where rapid urban growth and agricultural land transformation have occurred during the last three decades. In addition to presenting the methodological workflow, the chapter highlights key findings related to land-use change patterns, agricultural land loss, transition dynamics, and model performance. By linking methodological development with practical application, the proposed framework provides a transferable approach for investigating urban growth and future land-use change in different geographical contexts.

2. METHODOLOGICAL FRAMEWORK

The methodological framework presented in this chapter integrates remote sensing, Geographic Information Systems (GIS), multi-criteria evaluation, and statistical modelling techniques to investigate urban growth dynamics and future land-use change processes. Similar integrated approaches have been widely employed in land-use change modelling studies because they enable the simultaneous evaluation of environmental, accessibility-related, and demographic factors within a unified

analytical structure (Lesschen, Verburg, and Staal 2005; Veldkamp and Lambin 2001).

The modelling process follows a sequential structure in which the outputs of each stage serve as inputs for subsequent analyses. First, multi-temporal satellite imagery is processed to produce land use/land cover (LULC) maps using remote sensing techniques. Concurrently, explanatory variables associated with urban growth, including topographic, accessibility-related, land capability, and demographic factors, are prepared and standardized. Subsequently, variable weights are determined through the Analytic Hierarchy Process (AHP), and the most suitable variables are selected through Weighted Linear Combination (WLC) and Pearson correlation analyses. Finally, logistic regression is employed to estimate transition probabilities and generate future land-use scenarios. The primary objective of this framework is not only to identify historical land-use changes but also to explain the spatial factors driving these transformations and evaluate potential future development patterns. Figure 2.1 presents the general workflow of the methodological framework applied in this study.

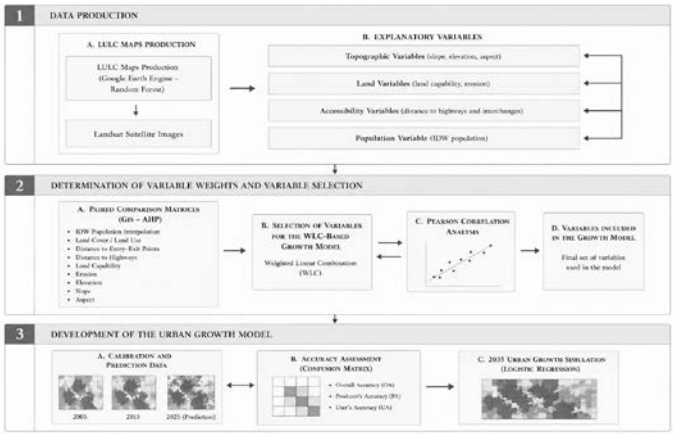

Figure 2.1 General workflow of the integrated urban growth modelling framework.

2.1. Study Area

The proposed framework was applied to the İzmir–Denizli Motorway corridor in western Türkiye. The study area consists of a 10-km buffer surrounding the motorway and its interchanges and covers portions of the provinces of İzmir, Aydın, and Denizli. Characterized by a mixture of built-up, agricultural, forest, and bare land classes, the corridor provides a suitable setting for examining the relationships between transportation infrastructure, land-use change, and urban growth dynamics

2.2. Data Preparation and LULC Mapping

The first stage of the framework involves the preparation of multi-temporal land use/land cover (LULC) datasets. Multi-temporal satellite imagery was employed to monitor land-use dynamics and provide the baseline information required for urban growth modelling. Landsat imagery was selected due to its long-term archive, consistent temporal coverage, and suitability for analysing long-term landscape transformations (Wulder et al., 2019).

Four reference years were used to represent the evolution of land-use patterns within the study area. Landsat 5 TM imagery was utilized for 1995, Landsat 7 ETM+ for 2005, and Landsat 8 OLI/TIRS imagery for 2015 and 2025. To minimize classification uncertainty, images with low cloud cover were selected and processed within the Google Earth Engine (GEE) environment (Gorelick et al. 2017).

Land-use classification was performed using the Random Forest (RF) algorithm, one of the most widely applied machine-learning methods in remote sensing studies due to its high classification accuracy and robustness when handling multi-source datasets (Belgiu and Drăgut 2016; Breiman 2001). Based on training samples collected for each reference year, RF models were developed to classify the imagery into five LULC

categories: built-up land, agricultural land, forest land, water bodies, and bare land.

To enhance spatial consistency among datasets, all classified maps and explanatory variables were converted to a common spatial resolution prior to analysis. The resulting LULC maps constitute the primary input for subsequent change detection and urban growth modelling procedures.

2.3. Variable Preparation and Selection

Urban growth is influenced by a combination of physical, accessibility-related, environmental, and demographic factors. Accordingly, a set of explanatory variables frequently employed in urban growth modelling studies was prepared and evaluated (Allen and Lu 2003; Hu and Lo 2007; Lesschen et al. 2005).

The initial variable pool consisted of nine variables representing different dimensions of urban development: slope, elevation, aspect, land capability, erosion risk, existing land use/land cover (LULC), population distribution, distance to the motorway, and distance to motorway interchanges. Topographic variables were derived from Digital Elevation Model (DEM) data, whereas land capability and erosion layers were obtained from national spatial datasets. Accessibility variables were generated using the motorway network and interchange locations.

Population distribution was represented through a continuous population surface produced using the Inverse Distance Weighting (IDW) interpolation technique. Unlike administrative population statistics, the resulting surface provides a spatially continuous representation of demographic pressure and enables the integration of population dynamics into raster-based modelling procedures.

All explanatory variables were converted into raster format and standardized to a common spatial resolution.

Subsequently, Weighted Linear Combination (WLC) and Pearson correlation analyses were applied to evaluate variable relationships and identify potential multicollinearity issues. Variables exhibiting strong correlations were carefully assessed to avoid redundancy within the modelling framework.

The final set of variables was determined based on their theoretical relevance, statistical performance, and contribution to explaining observed land-use transitions.

2.4. Urban Growth Modelling

The final stage of the framework involves the modelling of land-use transitions and the simulation of future development patterns. Urban growth modelling was conducted using logistic regression, a widely applied approach in land-use change studies due to its ability to quantify the relationships between observed land-use transitions and explanatory variables while maintaining a high degree of interpretability (Allen and Lu 2003; Hu and Lo 2007; Lesschen et al. 2005).

The modelling process consisted of three sequential steps: (i) variable weighting and selection, (ii) construction of the logistic regression model, and (iii) model validation. Together, these procedures enabled the identification of the main drivers of urban growth and the generation of future land-use scenarios.

2.4.1. Variable Weighting and Selection

To evaluate the relative importance of the explanatory variables, the Analytic Hierarchy Process (AHP) was employed. AHP provides a structured framework for comparing variables through pairwise evaluations and deriving relative weights based on expert knowledge and decision-making principles (Malczewski 1999; Saaty 1977).

The weighting procedure included nine variables: slope, elevation, aspect, land capability, erosion risk, existing land

use/land cover, population distribution, distance to the motorway, and distance to motorway interchanges. Pairwise comparisons were conducted using Saaty's nine-point scale, and consistency was assessed through the Consistency Ratio (CR). The resulting CR value remained within acceptable limits, indicating a satisfactory level of consistency among the comparisons.

The analysis revealed that population distribution, existing land-use conditions, and accessibility-related variables constituted the most influential factors within the modelling framework, whereas topographic variables generally received lower weights. These results provided a quantitative basis for variable prioritization and supported the subsequent selection of explanatory variables for logistic regression modelling.

To further reduce redundancy among variables, Pearson correlation analysis was performed following the AHP procedure. Correlation coefficients indicated moderate relationships between distance to motorway interchanges and distance to the motorway, as well as between slope and elevation. Consequently, the final variable set used in the logistic regression model consisted of three variables: population distribution (IDW), distance to motorway interchanges, and elevation. These variables were selected based on their relative importance, low inter-correlation, and ability to represent the primary demographic, accessibility, and physical dimensions of urban growth.

2.4.2. Logistic Regression Model Construction

Among the various approaches used to model land-use change, logistic regression remains one of the most widely adopted techniques due to its ability to quantify relationships between land-use transitions and explanatory variables while maintaining a high degree of interpretability (Allen and Lu 2003; Hu and Lo 2007; Wu and Yeh 1997).

The method estimates the probability that a spatial unit will experience a specific land-use transition. In urban growth studies, this transition is typically defined as the conversion of non-urban land into urban land. Consequently, logistic regression provides a probability-based representation of urban expansion and facilitates the identification of factors influencing development patterns.

Logistic regression requires a binary dependent variable. Therefore, land-use transitions are reclassified separately for each land-use category prior to model calibration.

For each target class, a binary transition map is generated in which:

- Cells that transition to the target land-use class are assigned a value of 1;
- Cells that do not transition to the target land-use class are assigned a value of 0.

This procedure is repeated for all land-use classes included in the analysis. The resulting binary datasets constitute the dependent variables used in the logistic regression models and enable the estimation of transition probabilities for each land-use category at the raster-cell level.

Logistic regression estimates the probability of urban transition using a nonlinear logistic function that relates the dependent variable to a set of explanatory variables. The general form of the logistic function is expressed as:

$$f(z) = \frac{1}{1 + e^{-z}}$$

where f(z) represents the probability of occurrence of the event of interest and z denotes the linear predictor.

In urban growth modelling, the probability that a raster cell will be converted to urban land is calculated as:

$$P\ (Y = 1|x_1, x_2, \dots, x_k) = \frac{1}{1 + e^{-(\alpha + \sum_{i=1}^{k} \beta_i x_i)}}$$

where:

- $P\ (Y = 1|x_1, x_2, \dots, x_k)$ is the probability of urban transition;
- α is the intercept term;
- β_i represents the regression coefficient associated with the i^{th} explanatory variable;
- x_i denotes the value of i^{th} explanatory variable;
- k is the total number of explanatory variables;
- e is the base of the natural logarithm.

The model produces a probability value ranging from 0 to 1 for each raster cell. Higher probability values indicate a greater likelihood of future urban development, whereas lower values represent a lower potential for urban transition (Hu and Lo 2007; Nong and Du 2011).

The modelling procedure was implemented using the Modules for Land Use Change Evaluation (MOLUSCE) plugin within the QGIS environment. MOLUSCE provides an integrated platform for analysing historical land-use changes, incorporating explanatory variables, calibrating logistic regression models, and generating future land-use scenarios. Historical LULC maps and the selected explanatory variables were jointly used to estimate transition probabilities and simulate future land-use patterns.

The primary output of the modelling process is a set of spatial probability surfaces representing the likelihood of transition for each land-use class. These probability maps indicate the relative susceptibility of individual raster cells to future land-

use change and provide a spatially explicit representation of development potential. Beyond their predictive function, probability surfaces offer valuable insights into the spatial structure of land-use dynamics and support the identification of areas exposed to future development pressure. Consequently, they constitute an important analytical output for land-use planning and decision-making processes.

2.4.3. Model Validation

Model performance was evaluated by comparing simulated land-use maps with observed land-use conditions for the corresponding reference year. Validation was conducted using a confusion matrix approach, which quantifies the agreement between simulated and observed land-use classes.

Table 3.1 presents the general structure of the confusion matrix employed in the validation procedure. The diagonal elements ((a), (f), (k), and (p)) represent correctly classified pixels, whereas the off-diagonal elements indicate misclassified pixels. The total number of observations is represented by (N). For each land-use class, the values of True Positive (TP), True Negative (TN), False Positive (FP), and False Negative (FN) can be derived from the confusion matrix and subsequently used to calculate class-specific and overall performance metrics.

Table 3.1 General structure of the confusion matrix.

Observed / Predicted	Built-up Land	Agricultural Land	Forest Land	Bare Land	Total
Built-up Land (Predicted)	a	b	c	d	a+b+c+d
Agricultural Land (Predicted)	e	f	g	h	e+f+g+h
Forest Land (Predicted)	i	j	k	l	i+j+k+l
Bare Land (Predicted)	m	n	o	p	m+n+o+p
Total	a+e+i+m	b+f+j+n	c+g+k+o	d+h+l+p	N

The diagonal elements ((a), (f), (k), and (p)) represent correctly predicted pixels, whereas the off-diagonal elements indicate misclassified pixels. For class-specific accuracy assessment, the values of True Positive (TP), True Negative (TN), False Positive (FP), and False Negative (FN) are derived separately for each land-use class from the confusion matrix. The total number of observations is represented by (N).

Based on the confusion matrix, Overall Accuracy (OA), the Kappa coefficient, Producer's Accuracy (PA), and User's Accuracy (UA) were calculated. Overall Accuracy measures the proportion of correctly classified cells relative to the total number of observations, whereas the Kappa coefficient evaluates agreement beyond chance (Cohen Jacob 1960). Producer's Accuracy and User's Accuracy provide class-specific assessments of omission and commission errors, respectively.

In addition to statistical indicators, spatial validation was performed to examine the geographical distribution of correctly and incorrectly predicted cells. This procedure enables the identification of spatial clusters of prediction errors and provides additional insights into the spatial reliability of model outputs.

The combined use of statistical and spatial validation measures allows for a comprehensive evaluation of model performance by assessing both numerical agreement and geographical consistency between simulated and observed land-use patterns.

3. FRAMEWORK APPLICATION

To demonstrate the applicability of the proposed methodology, the framework was implemented in the İzmir–Denizli Motorway corridor in western Türkiye. The study area provides an appropriate testing environment due to its long-term exposure to transportation investments, diverse land-use characteristics, and observable urban growth patterns.

The implementation process followed the methodological workflow presented in Figure 2.1. Multi-temporal satellite imagery was first used to generate LULC maps representing different stages of development within the corridor. Subsequently, explanatory variables describing topographic

conditions, accessibility characteristics, environmental suitability, and demographic dynamics were prepared and standardized within a GIS environment. Following variable weighting and selection procedures, logistic regression models were developed to estimate transition probabilities and simulate future land-use patterns.

The application demonstrated the capability of the framework to integrate heterogeneous spatial datasets within a single modelling environment. By combining remotely sensed observations with spatial explanatory variables, the framework enables the investigation of both historical land-use dynamics and the factors associated with urban growth processes. In addition, the modelling procedure allows the generation of spatially explicit probability surfaces that can support future land-use simulations and scenario development.

Rather than focusing exclusively on land-use change detection, the framework provides a broader analytical perspective by linking observed spatial transformations to demographic, accessibility-related, and environmental drivers. This integrated structure contributes to a more comprehensive understanding of urban growth processes and facilitates the identification of areas potentially exposed to future development pressure.

The outputs generated through the framework include multi-temporal LULC maps, explanatory variable layers, variable importance assessments, transition probability surfaces, model validation metrics, and future land-use scenarios. Together, these outputs provide a comprehensive basis for evaluating urban growth dynamics and supporting planning and land management decisions in transportation corridors.

3.1. Key Observations from the Application

The implementation of the proposed framework revealed several patterns that demonstrate its analytical capabilities. The generated LULC maps indicated substantial changes in land-use composition throughout the study period. Between 1995 and 2025, the proportion of built-up land increased from approximately 9% to 20% of the study area, while agricultural land decreased from 34% to 30%. Forest land exhibited a relatively limited decline from 31% to 29%, whereas bare land decreased from 26% to 21%.

The analysis further highlighted the role of accessibility and demographic dynamics in shaping urban growth patterns. Variable weighting and selection procedures consistently identified population distribution, accessibility to motorway interchanges, and elevation as influential factors explaining observed land-use transitions. These findings support the importance of integrating demographic, physical, and transportation-related variables within urban growth modelling frameworks.

In addition to quantifying overall land-use changes, the framework enabled the identification of broader transition dynamics. Results indicated that urban expansion frequently occurred through intermediate transformation stages rather than direct land-use conversion processes. Such patterns illustrate the capacity of the proposed framework to capture complex spatial transformation processes associated with transportation infrastructure development.

Model validation results demonstrated a satisfactory level of agreement between simulated and observed land-use patterns. Overall Accuracy values exceeded 80%, while Kappa statistics indicated substantial agreement, suggesting that the selected

modelling structure was capable of reproducing the major spatial trends observed within the study area.

These observations are presented solely to illustrate the analytical outputs generated by the framework. Detailed interpretation of land-use change patterns and their implications falls beyond the scope of this methodological chapter.

3.2. Planning Implications

Beyond its methodological contribution, the proposed framework provides practical insights for spatial planning and land management. The integration of remote sensing, GIS, demographic information, and transportation-related variables enables the identification of areas exposed to future development pressure and supports the evaluation of alternative growth scenarios.

Particularly in transportation corridors, where accessibility improvements frequently stimulate urban expansion, modelling outputs can assist planners in identifying vulnerable agricultural and natural areas before irreversible land-use changes occur. The framework also facilitates the assessment of potential interactions between transportation investments and surrounding land-use systems, contributing to more informed planning decisions.

Furthermore, the ability to generate spatially explicit probability surfaces offers valuable support for growth management strategies, agricultural land protection policies, and sustainable development initiatives. By linking observed land-use changes with their underlying drivers, the framework provides a basis for proactive planning approaches rather than reactive responses to ongoing urban expansion.

Although the methodology was demonstrated using the İzmir–Denizli Motorway corridor, its reliance on widely

available spatial datasets and transferable analytical procedures allows adaptation to different geographical contexts. Consequently, the framework may serve as a useful decision-support tool for researchers, planners, and policymakers concerned with urban growth and land-use change in transportation corridors.

4. CONCLUSION

This chapter presented an integrated framework for analysing urban growth and future land-use change in transportation corridors through the combined use of remote sensing, Geographic Information Systems (GIS), multi-criteria evaluation, and logistic regression modelling. By integrating multi-temporal LULC data with demographic, environmental, and accessibility-related variables, the framework provides a systematic approach for investigating the spatial processes underlying urban expansion.

The application conducted in the İzmir–Denizli Motorway corridor demonstrated the operational capacity of the framework to identify historical land-use dynamics, evaluate the factors associated with urban growth, and generate future land-use scenarios. The results confirmed the importance of accessibility and demographic variables in explaining observed land-use transformations and highlighted the potential of the framework for supporting planning and land management processes.

One of the principal strengths of the proposed approach is its reliance on widely accessible datasets and transferable analytical procedures. The use of Landsat imagery, digital elevation models, population data, and transportation network information allows the methodology to be implemented in different geographical contexts and at various spatial scales. Moreover, cloud-based processing environments facilitate

reproducibility and improve the efficiency of data processing and model development.

Despite these advantages, the framework remains dependent on the quality of available datasets and the selection of explanatory variables. Future studies may improve model performance through the incorporation of additional socioeconomic, institutional, and policy-related variables that influence urban growth dynamics.

Overall, the proposed framework offers a practical and replicable methodology for analysing land-use change and urban growth in transportation corridors. By combining remote sensing, GIS, and statistical modelling techniques within a unified analytical structure, it provides a valuable tool for both academic research and planning practice.

REFERENCES

Allen, Jeffery, and Kang Lu. 2003. 'Modeling and Prediction of Future Urban Growth in the Charleston Region of South Carolina: A GIS-Based Integrated Approach'. *Ecology and Society* 8(2). doi:10.5751/es-00595-080202.

Antrop, Marc. 2004. 'Landscape Change and the Urbanization Process in Europe'. *Landscape and Urban Planning* 67(1–4):9–26. doi:10.1016/S0169-2046(03)00026-4.

Baum-Snow, Nathaniel. 2007. 'Did Highways Cause Suburbanization?' *The Quarterly Journal of Economics* 122(2):775–805. https://academic.oup.com/qje/article-abstract/122/2/775/1942140.

Belgiu, Mariana, and Lucian Drăgut. 2016. 'Random Forest in Remote Sensing: A Review of Applications and Future Directions'. *ISPRS Journal of Photogrammetry and Remote Sensing* 114:24–31. doi:10.1016/j.isprsjprs.2016.01.011.

Breiman, Leo. 2001. 'Random Forests'. *Machine Learning* 45:5–32. doi:https://doi.org/10.1023/A:1010933404324.

Chi, Guangqing. 2010. 'The Impacts of Highway Expansion on Population Change: An Integrated Spatial Approach'. *Rural Sociology* 75(1):58–89. doi:10.1111/j.1549-0831.2009.00003.x.

Cohen Jacob. 1960. 'A Coefficient of Agreement for Nominal Scales'. *Educational and Psychological Measurement* 20(1):37–46.

Duranton, Gilles, and Matthew A. Turner. 2012. 'Urban Growth and Transportation'. *Review of Economic Studies* 79(4):1407–40. doi:10.1093/restud/rds010.

EEA. 2006. *Urban Sprawl in Europe — The Ignored Challenge.*

Copenhagen.

ESPON. 2020. *ESPON SUPER – Sustainable Urbanisation and Land-Use Practices in European Regions*.

Garcia-López, Miquel àngel. 2012. 'Urban Spatial Structure, Suburbanization and Transportation in Barcelona'. *Journal of Urban Economics* 72(2–3):176–90. doi:10.1016/j.jue.2012.05.003.

Gorelick, Noel, Matt Hancher, Mike Dixon, Simon Ilyushchenko, David Thau, and Rebecca Moore. 2017. 'Google Earth Engine: Planetary-Scale Geospatial Analysis for Everyone'. *Remote Sensing of Environment* 202:18–27. doi:10.1016/j.rse.2017.06.031.

Hu, Zhiyong, and C. P. Lo. 2007. 'Modeling Urban Growth in Atlanta Using Logistic Regression'. *Computers, Environment and Urban Systems* 31(6):667–88. doi:10.1016/j.compenvurbsys.2006.11.001.

Kasraian, Dena, Kees Maat, Dominic Stead, and Bert Van Wee. 2016. 'Long-Term Impacts of Transport Infrastructure Networks on Land-Use Change: An International Review of Empirical Studies'. *Transport Reviews* 36(6):772–92. doi:10.1080/01441647.2016.1168887.

Lambin, Eric F., and Patrick Meyfroidt. 2011. 'Global Land Use Change, Economic Globalization, and the Looming Land Scarcity'. *Proceedings of the National Academy of Sciences of the United States of America* 108(9):3465–72. doi:10.1073/pnas.1100480108.

Lesschen, Jan Peter, Peter H. Verburg, and Steven J. Staal. 2005. *Statistical Methods for Analysing the Spatial Dimension of Changes in Land Use and Farming Systems*. Vol. 7. http://scholar.google.com/scholar?hl=en&btnG=Search&q=intitle:Statistical+methods+for+analysing+the+spatial

+dimension+of+changes+in+land+use+and+farming+systems#0.

Lu, D., and Q. Weng. 2007. 'A Survey of Image Classification Methods and Techniques for Improving Classification Performance'. *International Journal of Remote Sensing* 28(5):823–70. doi:10.1080/01431160600746456.

Malczewski, Jacek. 1999. *GIS and Multicriteria Decision Analysis*. New York: John Wiley & Sons.

Müller, Kalin, Charlotte Steinmeier, and Meinrad Küchler. 2010. 'Urban Growth along Motorways in Switzerland'. *Landscape and Urban Planning* 98(1):3–12. doi:10.1016/j.landurbplan.2010.07.004.

Nong, Yu, and Qingyun Du. 2011. 'Urban Growth Pattern Modeling Using Logistic Regression'. *Geo-Spatial Information Science* 14(1):62–67. doi:10.1007/s11806-011-0427-x.

Saaty, Thomas L. 1977. 'A Scaling Method for Priorities in Hierarchical Structures'. *Journal of Mathematical Psychology* 15(3):234–81. doi:10.1016/0022-2496(77)90033-5.

Seto, Karen C., Burak Güneralp, and Lucy R. Hutyra. 2012. 'Global Forecasts of Urban Expansion to 2030 and Direct Impacts on Biodiversity and Carbon Pools'. *Proceedings of the National Academy of Sciences of the United States of America* 109(40):16083–88. doi:10.1073/pnas.1211658109.

Turner, B. L., Patrick Meyfroidt, Tobias Kuemmerle, Daniel Müller, and Rinku Roy Chowdhury. 2020. 'Framing the Search for a Theory of Land Use'. *Journal of Land Use Science* 15(4):489–508. doi:10.1080/1747423X.2020.1811792.

Veldkamp, A., and E. F. Lambin. 2001. 'Editorial: Predicting Land-Use Change'. *Agriculture, Ecosystems and Environment* 85(1–3):1–6. doi:10.1016/S0167-8809(01)00199-2.

Wu, Fulong, and Anthony Gar On Yeh. 1997. 'Changing Spatial Distribution and Determinants of Land Development in Chinese Cities in the Transition from a Centrally Planned Economy to a Socialist Market Economy: A Case Study of Guangzhou'. *Urban Studies* 34(11):1851–79. doi:10.1080/0042098975286.

Wu, Jianguo. 2019. 'Linking Landscape, Land System and Design Approaches to Achieve Sustainability'. *Journal of Land Use Science* 14(2):173–89. doi:10.1080/1747423X.2019.1602677.

Wulder, Michael A., Thomas R. Loveland, David P. Roy, Christopher J. Crawford, Jeffrey G. Masek, Curtis E. Woodcock, Richard G. Allen, Martha C. Anderson, Alan S. Belward, Warren B. Cohen, John Dwyer, Angela Erb, Feng Gao, Patrick Griffiths, Dennis Helder, Txomin Hermosilla, James D. Hipple, Patrick Hostert, M. Joseph Hughes, Justin Huntington, David M. Johnson, Robert Kennedy, Ayse Kilic, Zhan Li, Leo Lymburner, Joel McCorkel, Nima Pahlevan, Theodore A. Scambos, Crystal Schaaf, John R. Schott, Yongwei Sheng, James Storey, Eric Vermote, James Vogelmann, Joanne C. White, Randolph H. Wynne, and Zhe Zhu. 2019. 'Current Status of Landsat Program, Science, and Applications'. *Remote Sensing of Environment* 225(November 2018):127–47. doi:10.1016/j.rse.2019.02.015.

KENTSEL ULAŞIM AĞI TOPOLOJİSİ VE ERİŞİLEBİLİRLİK İLİŞKİSİ: TORBALI ÖRNEĞİ

Halil TOPÇU[1]

Umut ERDEM[2]

1. GİRİŞ

Erişilebilirlik, sadece toplumun günlük hareketliliğini değil, aynı zamanda afet veya acil durumlarda kritik hizmetlerin sürekliliğini de etkileyen kentsel sistemlerin temel boyutlarından biridir. Ulaşım ağlarının işlevliliği, sağlık, yeşil, afet toplanma alanları, kamusal ve diğer kentsel donatılara erişimi direkt etkilemektedir. Dolayısıyla yolların görece önemini ve kentsel ağlardaki rolünü anlamak, dirençli kent planı ve afet yönetimi bağlamında giderek önemli hale gelmiştir.

Kentsel ulaşım sistemleri, kentin genel erişilebilirliğini belirleyen birbirine bağlı yollar ve düğüm noktalarından oluşan karmaşık ağlardır. Stratejik olarak önemli yolların hasar alması ile, kent içi bölgelerin, hatta kentin diğer kentlerden izole olma durumu, gecikmiş acil müdahale, sağlık gibi kritik hizmetlere sınırlı erişim, afet gibi durumlarda ise tahliye / yardım operasyonlarının kesintiye uğraması da dahil olmak üzere ciddi sonuçlar ortaya çıkabilmektedir. Bu nedenle kritik yol segmentlerini belirlemek ve potansiyel kesinti akslarının savunmasızlıklarına karşı risk yönetimi hazırlamak esastır.

[1] Yüksek Lisans Öğrencisi, İzmir Demokrasi Üniversitesi, Mimarlık Fakültesi, Şehir ve Bölge Planlama Bölümü, ORCID: 0009-0009-3366-179X.

[2] Doçent, İzmir Demokrasi Üniversitesi, Mimarlık Fakültesi, Şehir ve Bölge Planlama Bölümü, ORCID: 0000-0001-9822-3605.

Önemli ve erişimi kapanma potansiyeli olan yolların tespit edilip, kentsel altyapı sistemlerinin sürekliliği ve esnekliği sağlanması için önlem alınması gerekmektedir. Bu bağlamda coğrafi bilgi sistemleri yazılımı olan ArcGIS, mekânsal ağ analizlerine ve ulaşım ağlarının erişilebilirlik performansının hesaplanmasına olanak sağlamaktadır (Miller, 1991). Buna ek olarak, Rhinocross (Rhino 8) ile "UNA Tools" (Urban Network Analyst) kentsel ağ analiz aracının entegre kullanımı, kentsel erişilebilirlik performansının değerlendirilmesinde kilit rol oynayabilmektedir. Bina, donatı ve yol ağı veri kümeleri ile gerçekleştirilen analizler ile hem kentsel erişilebilirlik eksiklikleri hem de kentsel fonksiyonların bağımlı olduğu ulaşım koridorları tespit edilebilir.

Çalışmanın amacı, kentsel yaşam alanındaki yol ağlarının önemini hesaplayarak, afet gibi olası bir acil durumda ulaşım ağının kırılganlığı tespit etmek, akabinde de önem derecesi yüksek, afet sonrası erişilebilirliği ise kritik yolları da referans alan afet yönetimi / acil müdahale planlarına katkıda bulunmaktır. Erişilebilirlik analizlerinden farklı olarak gerçekleştirilen yol önemi analizleri, Graf Teorisi'nden türetilmiş, Python temelli hesaplanmış ağ metrikleridir. Hesaplamada, yolların birbirine bağlanma sayıları, düğüm noktaları, cephe genişlikleri, uzunlukları ve kademeleri parametre olarak belirlenmiştir. Çalışma kapsamında referans alınan afet sonrası durum, depremdir. Dolayısıyla çalışmalara deprem simülasyonu eklenmiş, binaların enkaz yayılımları hesaplanarak olası afet sonrası kapanma riski olan yollar, önemli yollar ve düğüm noktaları tespit edilmiştir.

Tespit edilen önemli yollar toplam 209 adettir. Afet durumunda kapanan yollar ise 678 adetken, bu kapanan yolların 68'i (yaklaşık %10) önemli olarak tespit edilen yollardır. Dolayısıyla incelenen kullanımlara erişimde (hastane, aile sağlık merkezi, afet toplanma alanı, yeşil alan) ciddi oranda erişim kaybı yaşanmakta, kentin %70'lik bir kesimi izole kalmaktadır.

Dolayısıyla, tespit edilen önemli akslar referans alınarak, bir müdahale / afet yönetimi planı yapılması gereklidir. Aksi takdirde, yaşanacak olası bir afet sonrasında kent, ana ulaşım akslarını kaybetme, hizmetlere erişim sağlayamama, hem kent içi hem çeper kentlerle bir izolasyon sürecine girme riski taşımaktadır.

2. KENTSEL ERİŞİLİEBİLİRLİK VE AFET

Kentler, ulaşım gibi işlevsel altyapı ve sosyal bileşenlerin dinamik etkileşimine bağlı olduğu karmaşık sosyo-mekânsal sistemlerdir. Kentsel planlamada, mekânsal bağlantı ile afet riskini azaltma arasındaki bağ, kentsel dayanıklılığın temel parametrelerindendir. Bu bağlamda kentsel/mekânsal planlar, afet ve afet sonrası durum da referans alınarak gerçekleştirilmelidir.

2.1. Erişilebilirlik Nedir

Erişilebilirlik, belirli bir mekânsal sistemin etkileşim fırsatları ve potansiyelleri olarak tanımlanabilmektedir (Hansen, 1959). Erişilebilirlik farklı perspektiflerde değerlendirilebilmekle birlikte, ayrıca, belirli bir ulaşım modu (yaya, araç vs.) kullanılarak belirli bir konumdan herhangi bir fonksiyona ulaşmanın kolaylılığını da ifade etmektedir (Dalvi & Martin, 1976).

Kentsel planlamada erişilebilirlik, basit bir yakınlık kavramından ziyade, mekânın direncinin aşılmasıyla ilişkili, bir yerin doğasında olan bir özelliktir (Ingram, 1971). Bir mekânın erişilebilirliği, o mekânın işlevselliğini, fonksiyonelliğini ve potansiyelini de etkileyebilmektedir. Bu direnç ya da mekânsal engel ise, günlük hareketliliği kolaylaştırma konusundaki sistematik yeteneği belirlemektedir. Bu bakış açısı, odak noktasını mesafeden öteye taşımaktadır. Bu bağlamda modern

araştırmalar, erişilebilirliğin çok boyutlu olduğunu, arazi kullanımlarını, ulaşım olanaklarını, zamansal kısıtları ve bireysel ihtiyaçları entegre ettiğini savunmaktadır (Enderami ve ark, 2024; Geurs & van Wee, 2004). Dolayısıyla erişilebilirlik, toplumsal, sosyal ve ekonomik boyutlarıyla ele alınmalıdır. Erişilebilirliği tanımlamak için, ulaşım altyapısının toplumun sosyal ve ekonomik hedeflerini nasıl desteklediğine dair kapsamlı bir anlayış gerektirmektedir (Miller, 2018).

2.2. Afet Nedir

Afetler kentsel bağlam genelinde, yapılı çevre üzerinde yıkıcı etki potansiyeli taşıyan, düşük olasılıklı ve yüksek sonuçlu olaylar olarak sınıflandırılmaktadır (Koren & Rus, 2025). Bu tür olaylar, kentin omurgasında ani bir işlevsel şok teşkil eder. Bu şoklar genellikle, bir altyapı bileşeninin hasarlanması (genelde kentin ana aksı) ile sosyal ve ekonomik aksaklıklara yol açtığı zincirleme etkileri tetikleyebilmektedir (Wassmer, Merz & Marvan, 2024). Bu zincirleme reaksiyon, birbirine bağlı kentsel ağların aşırı kırılganlığını göstermektedir.

Sonuç olarak, bir afet sadece yapısal hasar durumu değil, kentin afeti sönümleme kapasitesini zorlayan, kritik hizmet akışlarının askıya alınması ve kentsel yaşamın aksamasıdır. Sönümleme kapasitesi, yani dirençlilik ise temel işlevlerin korunması, yedeklilik, kaynak ve hızlı iyileşme kavramlarının bileşkesi olarak değerlendirilebilmektedir (Bruneau ve ark, 2003). Bu olaylara yönelik planlama, uzun vadeli toplumun refahını sağlamak için belirsizlik senaryolarını yönetmeyi içermektedir (Tariverdi, Nunez-del-Prado, Leonova, & Rentschler, 2023). Proaktif yönetim sayesinde, kentsel sistemler bu tür feci şokların ardından iyileşme kabiliyetlerini artırabilmektedir.

2.3. Afet Durumunda Erişilebilirlik

Afet durumunda kentsel ağ, toplumun önemli bir kısmının hayati hizmetlere erişimini kaybetmesine neden olan ciddi bir parçalanma sürecine girebilmektedir. Afet olarak deprem referans alındığında, bina enkazları yol erişimini kısıtlayabilmekte ve etkilenen bölgelerin fiziksel olarak izole olmasına neden olabilmektedir (Koren & Rus, 2025). Bu fonksiyonel kırılganlık, enkaz yayılımının mevcut ağ topolojisini bozmasıyla ortaya çıkmaktadır (Golla, Bhattacharya & Gupta, 2020). Söz konusu fiziksel engeller, kentsel ağı birbirinden kopuk bağımsız elemanlara dönüştürerek temel hizmet düğüm noktalarını coğrafi olarak erişilemez hale getirebilmektedir (El-Maissi, Argyroudis, Kassem, Leong & Nazri, 2022). Ana arterlerin erişilemez olması, ağ topolojisini radikal oranda değiştirebilmekte, bir kesimi sistemden izole ederken afet sonrası iyileşme sürecini de etkileyebilmektedir. Bu bağlamda acil müdahale operasyonları için önemli yol aksı – mekânsal direnç ilişkisi maksimize edilerek fonksiyonel ve işlevsel kırılganlık değerlendirilmelidir.

Kentsel yaşamda stratejik öneme sahip yollar, kritik bir darboğaz haline dönüşebilmektedir (Wassmer ve ark., 2024). Stratejik bölgelerin izole olması, mekânsal empedansı artırmaktadır. Bu bağlamda ambulans ve yardım operasyonlarında gecikmeler meydana gelebilmektedir (Petricola, Reinmuth, Lautenbach, Hatfield, & Zipf, 2022; Rasulo, Nardoianni, Evangelisti, & D'Apuzzo, 2023). Bu kritik bağlantıların önceden tespit edilmesi, dirençli tahliye koridorlarının oluşturulması için temel bir gerekliliktir (Pei, Zhai, Hu, Liu, & Song, 2023). Mekânsal dirençteki bu artış, genellikle seyehat sürelerinin sıfıra ve sıfıra yakın seviyelere düştüğü ve yüksek yoğunluklu konut alanlarının izole olduğu "en kötü afet senaryolarına" neden olmaktadır. Dolayısıyla, yerel düzeydeki risklerin tespit edilmesi, büyük ölçekli sorunların önlenebilme potansiyelini artırmaktadır (Wassmer ve ark., 2024).

2.4. Bütünleşik Yaklaşımın Önemi

Kapsamlı afet yönetimi, hem fiziksel yapı hasarını hem de işlevsel ağ performansını entegre etmeyi gerektirmektedir. Bu entegrasyon, plancıların statik fiziksel değerlendirmelerin ötesine geçerek bir kentin sönümleme kapasitesini algılamalarını sağlar.

Mevcut müdahale – afet yönetim planlarının büyük çoğunluğu, afet durumunda ulaşım ağlarının kullanabileceğini referans alarak hazırlanmıştır. Oysa, afet sonrası durumda erişim kaybına uğrayan akslar olabilmektedir. Graf teorisine dayalı ölçütler (yol aksı ve düğüm noktaları) uygulanarak, afet öncesi erişim durumu ile afet sonrası - iyileşme sürecindeki erişim durumu karşılaştırılarak nicel olarak incelenebilmektedir. Böylesi bütüncül bir metodoloji, hasar görmüş ulaşım ağı içindeki gerçek zaman-maliyet kayıplarını yansıtan, izokronları haritalandırarak, hizmetlerden yeterince yararlanamayan bölgeleri tespit etmektedir. Dolayısıyla bu simülasyonlar, afet durumunda erişilebilirlik işlevini kaybeden yolların tespit edilmesine olanak sağlamaktadır. Bu bağlamda savunmasız kalabilecek kentsel bölgeler önceliklendirilerek, altyapı temelli bir risk sakınım planı veya bir revize bir kent planı yapılması gerekebilir.

3. METODOLOJİ

Çalışmalar, İzmir'in Torbalı ilçesinin kent merkezine odaklanmaktadır. Veri hazırlama, Python – VS Code – ArcGIS – Rhino yazılım temelli erişilebilirlik ve önem analizleri aşamalarından oluşan çalışma, afet risk yönetim planı, ulaşım planı ve müdahale operasyon planlarına somut katkı sunmayı hedeflemekte, dolayısıyla denetlenebilir ve benzer çalışmalara uygulanabilir olması amacıyla açık erişim kaynaklara dayanmaktadır.

3.1. Çalışma Alanı

Torbalı, son yıllarda hızlı nüfus artışı ve kentsel genişleme yaşayarak İzmir metropol bölgesinin önemli sanayi ve yerleşim alt merkezlerinden biri haline gelmiştir. İzmir'in 45 kilometre güneydoğusunda olan ilçe, önemli ulaşım koridorları üzerindeki stratejik konumu ve giderek gelişen fonksiyonel yoğunluğu nedeniyle, bölgesel erişilebilirliğin ve sosyo-ekonomik sürekliliğin sağlanmasında önemli bir rol oynamaktadır.

Torbalı seçilmesinin başlıca nedenlerinden biri, bölgenin çok sayıda doğal afete maruz kalması ve devam eden kentleşmeyle birlikte artan kırılganlığıdır. Bölgedeki aktif fay hatları, kentin kırsal çeperinde 3 – 4 metreye varan yarıklar açabilmektedir. Önceki çalışmalar, Torbalı'nın kalın alüvyon birikintileri ve düşük zemin taşıma kapasitesi ile karakterize olduğunu, bu koşulların sismik büyüme ve depreme bağlı hasara yatkınlığını artırdığını vurgulamaktadır (Demir & Karataş, 2024). Ayrıca ilçe, sel ve erozyon gibi afetlere maruz kalabilmekte ve dolayısıyla afete duyarlı planlama yaklaşımlarına ihtiyaç duyan bir bölgedir.

Afet riski barındıran ve stratejik ulaşım ağına sahip olan Torbalı, olası afet sonrası enkaz yayılımı ile kentin genel erişilebilirliğini kaybetmeye yatkın ilçedir. Dolayısıyla kent merkezi, erişilebilirlik, yol önem derecesi ve afet direnci arasındaki ilişkinin incelenebilmesi için önemli bir örnek teşkil etmektedir.

3.2. Veri

Veriler, dijital olarak toplanıp vektör veri halinde derlenmiştir. Erişilebilirlik ve çalışmanın ana odağı olan yol önem analizi için ihtiyaç duyulan yol ağı ve çalışmada "base-station" işlevleri gören bina kütleleri – donatılar, açık erişim Over Pass Turbo yazılımından tahsis edilmiştir. Çalışma alanı

içerisinde 2717 yol aksı, 7581 yapı kütlesi, 2 hastane, 9 aile sağlık merkezi, 35 yeşil alan ve 49 afet toplanma alanı mevcuttur.

3.3. Yöntem

Deprem, sel, heyelan ve benzeri afetler sonrasında sağlık hizmetleri, arama-kurtarma faaliyetleri, tahliye operasyonları ve lojistik destek süreçlerinin sürdürülebilirliği büyük ölçüde ulaşım ağlarının işlevselliğine bağlıdır. Bu nedenle, yol ağları içerisindeki kritik güzergâhların belirlenmesi ve yol önem derecelerinin ortaya konulması, ulaşım planlaması ve kentsel dayanıklılık çalışmalarında önemli bir araştırma alanı haline gelmiştir. Yol önem derecesinin belirlenmesi, yalnızca fiziksel özelliklerin değerlendirilmesiyle sınırlı olmayıp, aynı zamanda yol ağının topolojik yapısını ve kullanım karakteristiklerini de içeren çok kriterli bir yaklaşımı gerektirmektedir.

Çalışma kapsamında, yol önem derecesinin hesaplanmasında öncelikle çizgisel formatta bulunan yol verileri (line/.shp), Coğrafi Bilgi Sistemleri (CBS) ortamından elde edilerek Python programlama dili ve NetworkX kütüphanesi yardımıyla matematiksel bir ağ yapısına dönüştürülmektedir. Bu aşamada kod düzenleme ve komut girme işlevi için VS Code yazılımı çalışmaya dahil edilmiştir (Şekil 1). Oluşturulan ağ modeli sayesinde hem kavşak noktalarının hem de yol segmentlerinin ağ içerisindeki göreli önemleri merkeziyet ölçüleri yardımıyla değerlendirilebilmektedir.

Yol önem derecesinin belirlenmesinde kullanılan parametreler, ulaşım sisteminin hem yapısal hem de işlevsel özelliklerini temsil edecek şekilde seçilmektedir. Yol genişliği, acil durum araçlarının hareket kabiliyeti ve taşıma kapasitesi açısından önemli bir fiziksel kriter olarak değerlendirilirken yol uzunluğu ise ulaşım süreleri ve erişilebilirlik düzeyi üzerinde etkili olması nedeniyle analize dâhil edilmektedir. Ayrıca tercih

edilen yollar, günlük kullanım yoğunluğunu ve işlevsel önemi yansıtan parametreler olarak dikkate alınmaktadır.

Belirlenen parametreler normalize edilerek ağırlıklı bir değerlendirme modeli içerisinde bir araya getirilmektedir. Bu kapsamda ağ içerisindeki önem düzeyi yol genişliği %40, yol uzunluğu %35 ve tercih edilen aks ise %25 oranında ağırlıklandırılmaktadır. Bu ağırlıkların bir araya getirilmesi sonucunda her bir yol segmenti için 0 ile 1 arasında değişen bir yol önem skoru hesaplanmaktadır. Elde edilen yüksek önem değerleri, ilgili yol segmentlerinin ulaşım sistemi açısından stratejik bir konuma sahip olduğunu ve sistemin sürekliliği bakımından kritik rol oynadığını göstermektedir.

Gerçekleştirilen analiz sonucunda farklı amaçlara hizmet eden çeşitli veri katmanları üretilmektedir. İlk olarak, kavşak noktalarının ağ içerisindeki konumlarını ve merkeziyet özelliklerini gösteren düğüm katmanı oluşturulmaktadır. İkinci aşamada, yol segmentlerine ait önem derecelerini içeren çizgisel katman oluşturulmakta ve her bir yol için hesaplanan önem skorları öznitelik tablosuna aktarılmaktadır. Son olarak, önem değeri en yüksek olan yol segmentleri seçilerek kritik yol ağı katmanı elde edilmektedir. Bu katman, ulaşım sisteminin omurgasını oluşturan ve işlevselliğin sürdürülebilmesi açısından öncelikli olarak korunması gereken yolları temsil etmektedir.

4. BULGU

Bu çalışma kapsamında, Torbalı'nın kentsel ulaşım ağındaki önem – işlev hiyerarşisi, akabinde de olası afet (deprem) simülasyonunda kent içi erişilebilirliğin kırılganlığı analiz edilmiştir. Dijital veriler, ArcGIS, Rhinocross, VS Code yazılımlarının entegre kullanılması ile işlenmiştir (Şekil 1).

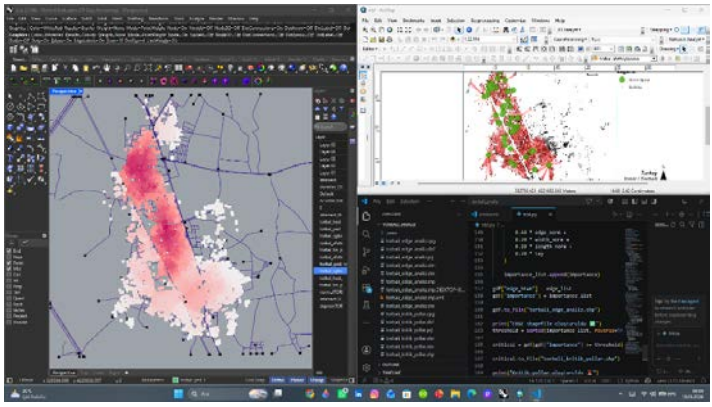

Şekil 1. Çalışma süreci yazılım kullanımı.

Not: Rhinocross, ArcGIS, VS Code.

Çalışmanın birincil odağı, yol önem derecelerini tespit etmektir. Bu bağlamda analizler gerçekleştirilip deprem simülasyonu kurgulanmıştır.

Yol önem derecesi analizi sonucu, kent içerisinde, alanın yoğun trafik akışını üstlenen 209 dilimden oluşmak üzere 7 ana aks tespit edilmiştir (Şekil 2). Bu akslar, kent merkezi olarak nitelendirilebilen "Torbalı Belediye Meydanı" etrafında bir çeper oluşturmaktadır.

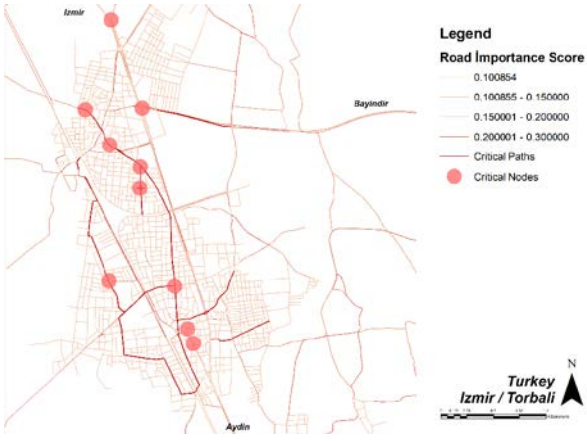

Şekil 2. Yol önem derecesi.

Not. Yazarlar tarafından Python, VS Code, ArcGIS ortamında üretilmiştir.

Deprem simülasyonu, binaların kat adetlerine göre enkaz yayılım çapının hesaplanması ile (h/2), yolların kapanma durumu referans alınarak, ilgili yolların network veri setinden çıkarılmasıyla gerçekleştirilmiştir (Şekil 3). Bu senaryoda kapanan yollar arasında, "önemli" olarak nitelendirilen aksların mevcutluğu kontrol edilmiştir.

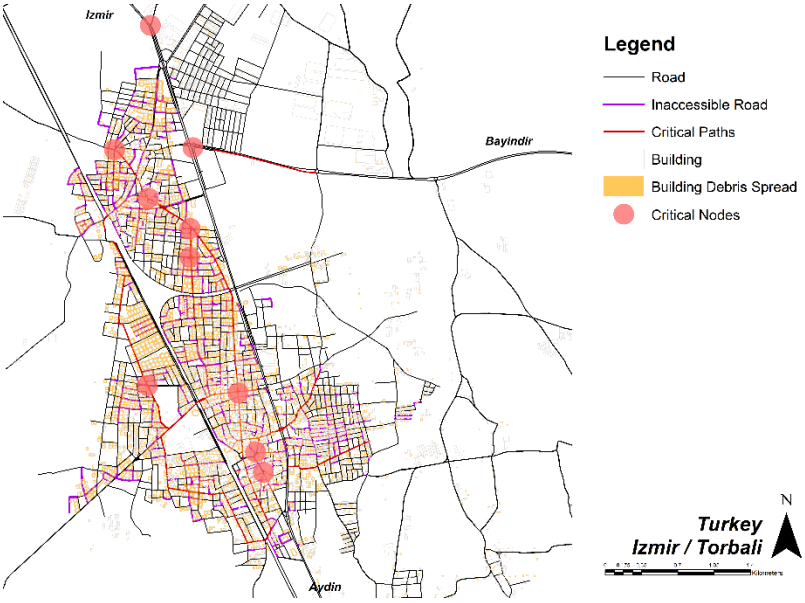

Şekil 3. Afet senaryosu ve yol ağı durumu.

Not. Yazarlar tarafından ArcGIS ortamında üretilmiştir.

Çalışma alanına afet olarak deprem simüle edildiğinde, gerek yüksek katlı binaların yoğunluğu gerek önemli ulaşım akslarının bu bölgeler çeperinde oluşu sebebiyle, kent içi ulaşım ağının %25.2'si erişilemez hale gelmektedir. Bu sayı, mevcut ulaşım ağının içerisindeki erişime kapanan yolların sayısıdır (2717 yol aksından 685'i). Dolayısıyla, kent içi genel erişim %70.8'lik bir kayba maruz kalmaktadır. Afet öncesi genel erişim, ArcGIS ve Rhinocross yazılım temelli gerçekleştirilen ağ analizleri paralelinde Şekil 4, 5, 6, 7'deki gibidir.

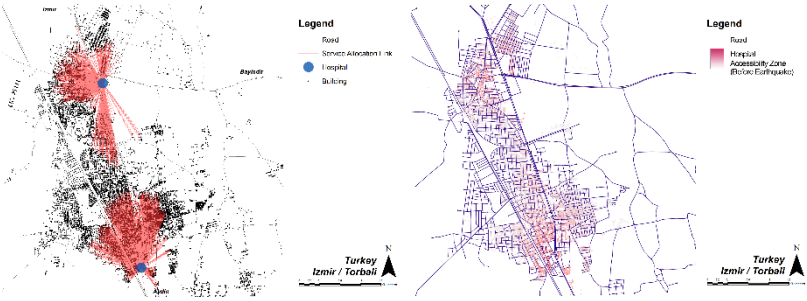

Şekil 4. Hastane erişilebilirliği.

Not. Yazarlar tarafından ArcGIS (sol görsel) ve Rhinocross (sağ görsel) ortamında üretilmiştir.

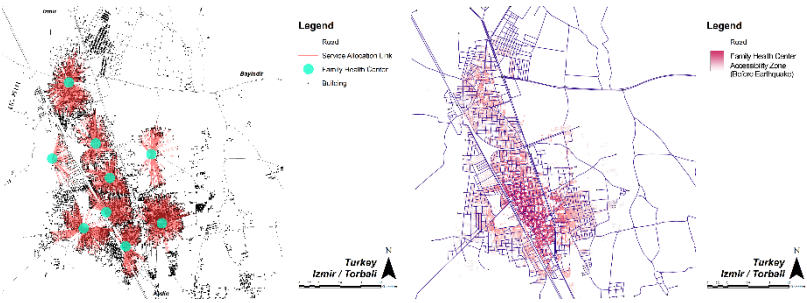

Şekil 5. Aile sağlık merkezi erişilebilirliği.

Not. Yazarlar tarafından ArcGIS (sol görsel) ve Rhinocross (sağ görsel) ortamında üretilmiştir.

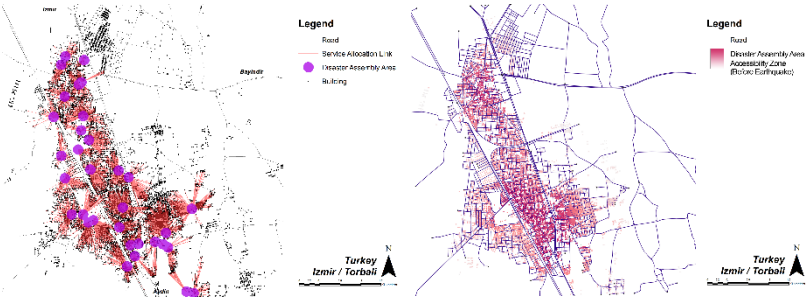

Şekil 6. Afet toplanma alanı erişilebilirliği.

Not. Yazarlar tarafından ArcGIS (sol görsel) ve Rhinocross (sağ görsel) ortamında üretilmiştir.

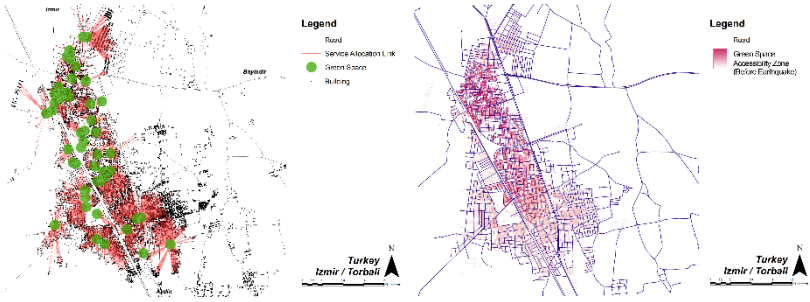

Şekil 7. Yeşil alan erişilebilirliği.

Not. Yazarlar tarafından ArcGIS (sol görsel) ve Rhinocross (sağ görsel) ortamında üretilmiştir.

Afet enkazında, tespit edilen önemli yollardan 67'si erişime kapanmıştır. Bu yollar, kent içi ulaşım yükünü karşılamasının yanı sıra, diğer yol akslarını da birbirine bağlamaktadır. Dolayısıyla, kent içi erişim kaybı, 67'yol diliminden (yaklaşık yol ağının %25.2'si) çok daha fazla olduğu tespit edilmiştir. Afet sonrası erişim kaybını ortaya koyan analizler Şekil 8, 9, 10, 11'de sunulmuştur.

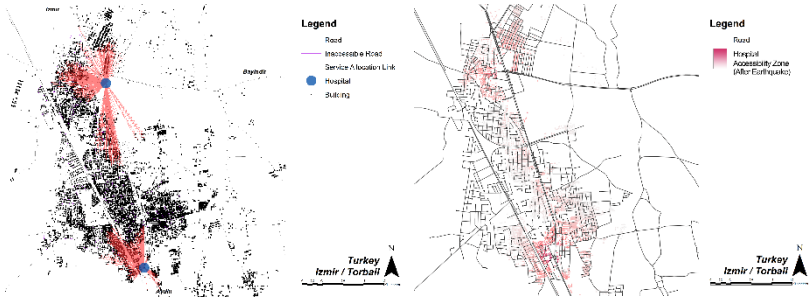

Şekil 8. Afet sonrası hastane erişilebilirliği.

Not. Yazarlar tarafından ArcGIS (sol görsel) ve Rhinocross (sağ görsel) ortamında üretilmiştir.

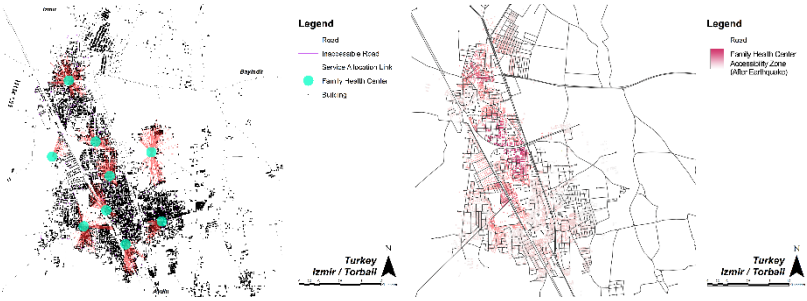

Şekil 9. Afet sonrası aile sağlık merkezi erişilebilirliği.

Not. Yazarlar tarafından ArcGIS (sol görsel) ve Rhinocross (sağ görsel) ortamında üretilmiştir.

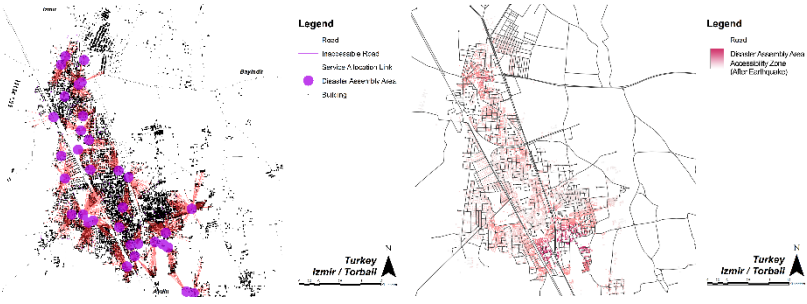

Şekil 10. Afet sonrası afet toplanma alanı erişilebilirliği.

Not. Yazarlar tarafından ArcGIS (sol görsel) ve Rhinocross (sağ görsel) ortamında üretilmiştir.

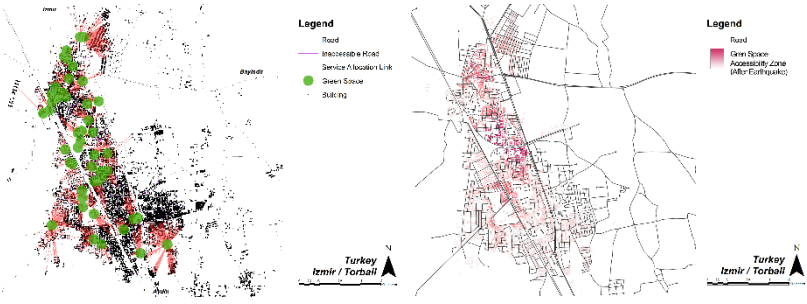

Şekil 11. Afet sonrası yeşil alan erişilebilirliği.

Not. Yazarlar tarafından ArcGIS (sol görsel) ve Rhinocross (sağ görsel) ortamında üretilmiştir.

Analizler, yapı bazlı erişim olarak kurgulanmış, bu bağlamda 7581 yapının, 3457'si hastaneye erişim sağlarken afet sonrası bu sayı 1430 yapıya düşmüştür. Bu sayılar aile sağlık merkezinde 5205'ten 1991, afet toplanma alanlarında 6140'tan 4146 ve yeşil alanlara erişimde 5921'den 3838 yapı şeklinde tespit edilmiştir. Erişim kaybının, kent geneline yayıldığı gözlemlenirken, merkez mevkiinin diğer bölgelere kıyasla dirençli olduğu tespit edilmiştir. Kent içi erişim kaybının radikal düzeyde olma sebebi, önemli yol akslarının, stratejik konumda yer alması, kent içi ulaşımı taşıma görevini üstlenmesindendir.

5. SONUÇ VE TARTIŞMA

Çalışmada, "Kentsel ulaşım ağında işlevsel bir hiyerarşi var mı, afet durumunda bu aksların hasar alıp erişilemez hale gelmesi durumunda kent içi kritik kullanımlara erişim nasıl şekillenir?" sorusuna yanıt aranmıştır. Çalışmanın bulguları, Torbalı'nın kent merkezine hizmet eden 7 ana önemli yol aksının olduğunu ortaya koymaktadır. Bu akslar dilim olarak değerlendirildiğinde ise 209 adettir. Yol önem derecesi analizleri paralelinde tespit edilen bu akslar, bilinen yol kademelenmesi haricinde düğüm, bağlantı sayıları, tercih edilebilirlik oranları gibi nitelikler sebebiyle kent içi ulaşım ağının omurgası niteliğindedir. Bulgular, önemli olarak tespit edilen aksların %10'unun erişim kaybına uğrayabileceğini, dolayısıyla kent içi ulaşım tipolojisinin ani şok sonucu radikal oranda değişebileceğini göstermektedir.

Elde edilen sonuçlar, afet yönetimi, acil durum lojistiği, tahliye planlaması, kritik altyapı yönetimi, sağlık hizmetlerine erişilebilirlik analizleri, arama-kurtarma faaliyetleri ve ulaşım sistemlerinin dayanıklılık değerlendirmeleri gibi birçok alanda kullanılabilmektedir. Özellikle deprem sonrası senaryolarda, yüksek önem derecesine sahip yolların açık tutulması, enkaz

kaldırma çalışmalarında öncelikli olarak değerlendirilmesi ve alternatif güzergâhların belirlenmesi açısından bu tür analizler önemli katkılar sağlamaktadır. Bunun yanı sıra, ağ teorisi ile coğrafi bilgi sistemlerinin bütünleşik kullanımına dayanan bu yaklaşım, kentlerin ulaşım dayanıklılığının değerlendirilmesi ve gelecekteki planlama süreçlerinde kritik koridorların belirlenmesi amacıyla kullanılabilecek kapsamlı bir karar destek mekanizması sunmaktadır.

KAYNAKÇA

Alğın Demir, K., & Karataş, N. (2024). Afet Olgusunun Zamansal ve Mekansal Boyutunun Kent Planlama Ekseninde Değerlendirilmesi: Torbalı İlçesi. Türk Deprem Araştırma Dergisi, 6(1), 98-122. doi:10.46464/tdad.1405733

Bruneau, M., Chang, S. E., Eguchi, R. T., Lee, G. C., O'Rourke, T. D., Reinhorn, A. M., ... & Von Winterfeldt, D. (2003). A framework to quantitatively assess and enhance the seismic resilience of communities. *Earthquake Spectra*, 19(4), 733–752. doi:10.1193/1.1623497

Dalvi, M. Q., & Martin, K. M. (1976). The measurement of accessibility: Some preliminary results. *Transportation*, 5(1), 17–42. doi:10.1007/bf00165245

El-Maissi, A. M., Argyroudis, S. A., Kassem, M. M., Leong, L. V., & Nazri, F. M. (2022). An integrated framework for the quantification of road network seismic vulnerability and accessibility to critical services. *Sustainability*, 14(19), 12474. doi:10.3390/su141912474

Enderami, S. A., Sutley, E., Helgeson, J., Dueñas-Osorio, L., Watson, M., & van de Lindt, J. W. (2024). Measuring post-disaster accessibility to essential goods and services: Proximity, availability, adequacy, and acceptability dimensions. *Journal of Infrastructure Preservation and Resilience*, 5, 12. doi:10.1186/s43065-024-00104-0

Geurs, K. T., & van Wee, B. (2004). Accessibility evaluation of land-use and transport strategies: Review and research directions. *Journal of Transport Geography*, 12(2), 127–140. doi:10.1016/j.jtrangeo.2003.10.005

Golla, A. P. S., Bhattacharya, S. P., & Gupta, A. (2020). The accessibility of urban neighborhoods when buildings

collapse due to an earthquake. *Transportation Research Part D: Transport and Environment*, 86, 102439. doi:10.1016/j.trd.2020.102439

Hansen, W. G. (1959). How accessibility shapes land use. *Journal of the American Institute of Planners*, 25(2), 73–76. doi:10.1080/01944365908978307

Ingram, D. R. (1971). The concept of accessibility: A search for an operational form. *Regional Studies*, 5(2), 101–107. doi:10.1080/09595237100185131

Koren, D., & Rus, K. (2025). Impact of earthquake-induced building debris on urban network functionality and citizen accessibility to urban functions. *Frontiers in the Built Environment*, 11, 1602963. doi:10.3389/fbuil.2025.1602963

Miller, E. J. (2018). Accessibility: Measurement and application in transportation planning. *Transport Reviews*, 38(5), 551–555. doi:10.1080/01441647.2018.1492778

Miller, H. J. (1991). Modelling accessibility using space-time prism concepts within geographical information systems. *International Journal of Geographical Information Systems*, 5(3), 287–301. doi:10.1080/02693799108927856

Petricola, S., Reinmuth, M., Lautenbach, S., Hatfield, C., & Zipf, A. (2022). Assessing road criticality and loss of healthcare accessibility during floods: The case of Cyclone Idai, Mozambique 2019. *International Journal of Health Geographics*, 21(1), 14. doi:10.1186/s12942-022-00315-2

Rasulo, A., Nardoianni, S., Evangelisti, A., & D'Apuzzo, M. (2023). Incorporating traffic models into seismic damage analysis of bridge road networks: A case study in Central

Italy. *Infrastructures*, 8(7), 113. doi:10.3390/infrastructures8070113

Tariverdi, M., Nunez-del-Prado, M., Leonova, N., & Rentschler, J. (2023). Measuring accessibility to public services and infrastructure criticality for disasters risk management. *Scientific Reports*, 13(1), 1661. doi:10.1038/s41598-023-28460-z

Wassmer, J., Merz, B., & Marwan, N. (2024). Resilience of transportation infrastructure networks to road failures. *Chaos: An Interdisciplinary Journal of Nonlinear Science*, 34(1), 013124. doi:10.1063/5.0165839

RISK ASSESSMENT AND RESILIENCE EVALUATION OF INTERIOR FINISHING MATERIALS IN EARTHQUAKE-PRONE RESIDENTIAL BUILDINGS: AN AHP–ENTROPY MULTI-CRITERIA ANALYSIS IN TEHRAN

Ali KEMER[1]

1. INTRODUCTION

Earthquakes rank among the most devastating natural disasters facing densely populated cities globally. Tehran, home to over 9.5 million people, is considered one of the world's most seismically hazardous capitals, surrounded by the North Tehran, Mosha, and Rey Faults. Geophysical estimates suggest a maximum credible earthquake of Mw 7.5–7.8 could occur on any of these faults within the coming century. Past Iranian earthquakes — including the 1990 Manjil–Rudbar (Mw 7.4), 2003 Bam (Mw 6.6), and 2017 Sarpol-e Zahab (Mw 7.3) — have starkly illustrated the toll of insufficient seismic preparedness in residential construction.

Recent scholarship in earthquake engineering has broadened its focus beyond structural collapse to encompass non-structural components (NSCs), which constitute 60–80% of total building value in modern residences and account for the majority of casualties in moderate seismic events. Interior finishing materials — including ceramic tiles, gypsum board systems,

[1] Dr. Öğr. Gör. İstanbul Aydin University, Department of Interior Architecture, ORCID: 0009-0000-4417-3948.

suspended ceilings, partition glazing, timber veneers, and decorative stone cladding — represent a notably understudied subset of NSCs. When these materials fail during earthquakes, they create projectile hazards, block evacuation routes, cause secondary injuries, and often render structurally intact buildings uninhabitable.

Yet Iranian building regulations, chiefly Standard 2800 (4th Edition), focus predominantly on structural elements, offering minimal prescriptive guidance on interior material selection for seismic contexts. This gap is further widened by a construction market where interior material choices are typically driven by aesthetics and cost over seismic performance — a pattern well-documented across the Global South.

Multi-Criteria Decision Analysis (MCDA) has gained traction as a robust approach to complex decision-making in the built environment, enabling simultaneous assessment of technical, economic, and safety-related criteria. The Analytic Hierarchy Process (AHP), developed by Saaty, offers a structured pairwise comparison method for deriving criterion weights from expert input. The Entropy-based weighting method, rooted in Shannon's information theory, complements AHP by extracting objective weights from data variability, thereby reducing subjective bias. Their hybrid combination — referred to here as AHP–Entropy MCDA — synthesises expert knowledge with empirical evidence and is increasingly applied in construction material evaluation.

This paper fills an identified research gap by applying an AHP–Entropy MCDA framework to evaluate the seismic risk and resilience of seven commonly used interior finishing materials in Tehran's residential buildings. Three objectives guide the study: (i) developing a comprehensive multi-criteria risk index for interior materials under seismic conditions; (ii) identifying

materials with the highest composite risk profiles in Tehran's housing stock; and (iii) offering evidence-based recommendations for material standards, retrofit policies, and indoor environment guidelines in earthquake-prone urban settings.

The paper proceeds as follows: Section 2 reviews literature on the seismic performance of non-structural interior components and MCDA applications in building material assessment. Section 3 outlines the study context, data collection, and modelling approach. Section 4 presents quantitative results including criterion weights, risk indices, and resilience rankings. Section 5 discusses findings and policy implications, and Section 6 addresses limitations and future research directions.

2. LITERATURE REVIEW

2.1. Seismic Vulnerability of Non-Structural Interior Components

Research into earthquake-induced non-structural damage grew significantly following post-event investigations of the 1994 Northridge and 1995 Kobe earthquakes, which showed that NSC failures were responsible for 75–82% of direct economic losses in residential and commercial buildings. Within this category, interior finishing materials have received far less systematic attention than mechanical, electrical, and plumbing (MEP) systems, which have been more thoroughly characterised through fragility analyses.

Taghavi and Miranda developed an influential classification of NSC vulnerabilities, grouping interior finishes by their damage-initiation acceleration thresholds. Their fragility analysis found that heavy ceramic wall and floor tiles begin to sustain damage at peak floor accelerations (PFA) as low as 0.15g–

0.20g — well below the design spectra for high-seismic zones. Experimental work by Petrone et al. corroborated these findings, showing that tile-adhesive bond failure depends not only on acceleration magnitude but also on inter-storey drift ratios (IDR) and ground motion cycling frequency. Drift-sensitive systems such as lightweight partition cladding and suspended ceiling grids have been shown to exhibit brittle failure at IDR values of 0.3–0.5%, within the operational performance targets of current seismic codes.

In the Iranian context, Hosseini and Hosseini surveyed damage following the 2012 Ahar–Varzaghan earthquake sequence, recording widespread ceramic tile failures in structurally undamaged residential buildings. Their work highlighted a critical gap between structural performance objectives and post-earthquake habitability — a distinction central to the present study. Zare and Hamzehloo subsequently characterised Tehran's residential building stock as largely composed of pre-2000 masonry and reinforced concrete frame structures, many of which lack seismic detailing in line with current Standard 2800, further heightening interior finish vulnerability across the city.

Component-level investigations have also shed light on specific interior systems. Magliulo et al. examined suspended ceiling grids under shake-table loading and identified grid connection failure as the primary collapse mechanism above IDR values of 0.5%. Dhakal documented non-structural interior damage following the 2010 Darfield earthquake, noting that partition and ceiling systems failed in buildings with no measurable structural loss — reinforcing the need for interior material risk frameworks that are independent of structural vulnerability models.

2.2. Indoor Environment Quality and Post-Seismic Material Hazards

The relationship between seismic performance and indoor environment quality (IEQ) is an emerging research area of direct relevance to this study. Fisk and subsequent meta-analyses have established clear links between interior material quality and occupant health under normal conditions, including VOC emissions, particulate matter, and moisture-driven mould. However, seismic events introduce acute IEQ hazards through material fragmentation, dust release, and HVAC system disruption — pathways that remain poorly characterised in the literature.

Asbestos-containing materials (ACMs), historically common in Iranian residential construction prior to the 1990s, pose a particular concern: seismic disruption can release chrysotile fibres, creating acute inhalation risks for occupants and emergency responders. Even modern, non-asbestos materials carry post-seismic IEQ risks — ceramic tile fragmentation generates respirable crystalline silica dust, classified as a Group 1 carcinogen by the IARC; disrupted gypsum board can release sulphur compounds in humid conditions; and fractured mineral wool ceiling tiles shed respirable ceramic fibres. These material-specific post-earthquake IEQ consequences have not been incorporated into existing seismic risk frameworks for residential interiors, representing a key gap this study addresses.

Drawing on the WHO Housing and Health Guidelines and the WELL Building Standard's material transparency provisions, this study includes IEQ impact as an explicit criterion within the MCDA framework — enabling simultaneous optimisation of seismic performance and occupant health, a dual-objective approach absent from prior seismic material assessment literature.

2.3. Multi-Criteria Decision Analysis in Built-Environment Material Assessment

MCDA methods have been increasingly adopted in construction material selection research to systematically integrate diverse performance criteria spanning technical, economic, environmental, and human-centred dimensions. Among available instruments, AHP has been most widely applied due to its theoretical clarity, computational accessibility, and compatibility with expert elicitation. Applications in the built environment include material selection for low-energy buildings, green building certification, and acoustic performance optimisation of interior wall systems.

The Entropy weighting method, grounded in Shannon's information theory, assigns criterion weights inversely proportional to the uniformity observed in the decision matrix, thereby prioritising criteria with stronger discriminatory power across alternatives. The diversification degree, $d_j = 1 - E_j$, captures each criterion's information content relative to the alternatives being evaluated. The hybrid combination of AHP and Entropy weights — variously described as integrated or compound weighting — has demonstrated superior discriminatory performance compared to either method used alone in recent construction material evaluation studies.

Within the seismic risk domain, MCDA has been applied to building-level vulnerability assessment, post-earthquake rapid visual screening, and urban-scale retrofit prioritisation. Zavadskas et al. provide a comprehensive review of MCDA applications in construction research, noting a growing trend towards hybrid weighting approaches that blend subjective and objective weight derivation. To the best of the authors' knowledge, however, no prior study has applied a hybrid AHP–Entropy framework specifically to evaluate the risk and resilience

of interior finishing materials in a high-seismicity metropolitan area. This study therefore occupies a novel position at the intersection of seismic risk assessment, indoor environmental quality research, and MCDA methodology.

3. STUDY CONTEXT AND SAMPLING FRAMEWORK

This stratified district selection ensures representation across the principal residential typologies found in Tehran, consistent with sampling approaches used in comparable urban seismic risk studies.

A total of 245 residential units were sampled across three districts: 87 in District 3, 91 in District 5, and 67 in District 22. Units were selected through stratified random sampling within each district, stratified by building height (low-rise: ≤4 storeys; mid-rise: 5–12 storeys; high-rise: >12 storeys) and construction period (pre-1990, 1990–2005, post-2005). All participating units were owner-occupied residential dwellings; survey access was arranged through Tehran Municipality building permit records. Ethical approval for field surveys and expert interviews was granted by the University of Tehran Institutional Review Board (Reference: UT-IRB-2023-0147), and written informed consent was obtained from all participants prior to their involvement.

3.1. Interior Finishing Materials Evaluated

Seven interior finishing material categories were identified as the primary alternatives (A_1–A_7) for evaluation. These were selected based on their documented prevalence in Tehran's residential building stock, as confirmed through pre-survey visual inspections and corroborated by Iranian construction industry market reports. Table 1 provides a descriptive overview of each material category, including

installation context, typical thickness, and approximate market prevalence among the sampled units.

Table 1. Interior Finishing Material Alternatives Evaluated in the Study

Code	Material Category	Description / Installation Context	Primary Location	Thickness (mm)	Prevalence (%)
A_1	**Ceramic Floor Tiles**	High-density fired clay tiles adhered with cement mortar or polymer-modified adhesive to the concrete sub-floor	Floors, wet areas	8–12	94.3
A_2	**Ceramic Wall Tiles**	Glazed ceramic tiles adhered to masonry or gypsum board substrates with cementitious adhesive	Bathrooms, kitchens	6–10	88.2
A_3	**Gypsum Plasterboard**	Single or double-layer 12.5 mm boards on lightweight cold-formed steel framing	Partitions, ceilings	12.5–25	76.7
A_4	**Suspended Acoustic Ceiling Tiles**	Mineral wool or fibre-reinforced gypsum tiles in braced T-bar grid systems per EN 13964	Living areas	15–25	58.4
A_5	**Decorative Stone/Marble Cladding**	Travertine or marble panels adhered to masonry walls with epoxy or cementitious adhesive.	Lobbies, entrance	20–40	42.1
A_6	**Lightweight Timber Wall Veneer**	Engineered wood panels or MDF veneer adhered to internal substrates	Living rooms	12–18	35.9
A_7	**Partition Glazing Systems**	Frameless or framed glass partitions (tempered or laminated) in aluminium profiles	Open-plan areas	10–15	28.6

(n = 245 residential units, Tehran)

3.2. Evaluation Criteria

Seven evaluation criteria (C_1–C_7) were established through a systematic literature review and an iterative Delphi consultation with a panel of 18 domain experts, comprising seismic engineers (n = 6), building material scientists (n = 4),

indoor environment quality specialists (n = 4), and practising architects with seismic retrofit experience (n = 4). The Delphi process ran over three rounds, reaching consensus — defined as an interquartile range of ≤1.0 on a 1–5 Likert scale by the third round — in line with established Delphi protocols for built-environment research. Table 2 presents each criterion's definition, measurement basis, and optimality direction (benefit: higher is better; cost: lower is better).

Table 2. Evaluation Criteria for AHP–Entropy Multi-Criteria Assessment of Interior Finishing Materials

Code	Criterion	Definition and Measurement Basis	Unit	Direction	Data Source
C_1	**Seismic Fragility Index**	Probability of moderate-to-severe damage at PFA = 0.3g, derived from fragility curve analysis calibrated against the Tehran ground motion dataset and supplemented by expert Delphi scoring	0–1 (norm.)	Cost	Fragility curves; Delphi
C_2	**Fire Resistance Rating**	Duration (hours) of fire resistance to ISO 834 standard fire curve penetration, per EN 13501-1 classification records and product datasheets	Hours	Benefit	EN 13501-1; datasheets
C_3	**Impact Resistance**	Peak force (kN) sustained without fracture per EN 13116 pendulum impact test; lab-tested at Sharif University Materials Laboratory	kN	Benefit	EN 13116; lab tests
C_4	**Occupant Injury Potential**	Composite injury hazard index accounting for fragmentation behaviour, sharp-edge generation, and mass-over-area ratio at failure	0–1 (norm.)	Cost	Expert Delphi; literature
C_5	**Post-Earthquake Replaceability**	Expert-rated ease and speed of material replacement within a 72-hour emergency window; scaled 1–5 (1 = very difficult, 5 = very easy)	Scale 1–5	Benefit	Expert Delphi (n = 18)
C_6	**IEQ Impact (Post-Seismic)**	Index of indoor air quality degradation potential following material fragmentation, including silica dust, VOC release, and fibre liberation	0–1 (norm.)	Cost	Literature; chamber testing
C_7	**Life-Cycle Cost (Seismic Scenario)**	Annualised expected cost of repair/replacement per unit area at a 475-year return period seismic hazard level, based on HAZUS-MH adapted for Tehran cost database	USD/m²/yr	Cost	HAZUS; quantity surveyor

3.3. AHP Pairwise Comparison and Weight Derivation

AHP criterion weights were derived following Saaty's established pairwise comparison protocol. Each of the 18 panel members completed a pairwise comparison matrix for the seven criteria using Saaty's 1–9 integer scale, where 1 indicates equal importance and 9 indicates extreme importance of one criterion over another. Individual matrices were aggregated using the geometric mean of each cell — the recommended technique for group AHP judgements — to produce a consolidated group comparison matrix. The normalised principal eigenvector of this matrix formed the AHP weight vector (w_j^{AHP}). Consistency was assessed using the Consistency Ratio (CR):

$$\mathbf{CR = CI / RI}$$

$$CI = (\lambda max - n) / (n - 1)$$

where CI is the Consistency Index, λmax is the principal eigenvalue, n = 7 is the matrix order, and RI is the Random Index (RI_7 = 1.32).15 A CR threshold of 0.10 was adopted as the acceptability criterion. All group pairwise matrices yielded CR values below this threshold (CR = 0.083), confirming acceptable consistency and validating the expert judgements for use in subsequent weight calculations.

3.4. Entropy-Based Objective Weighting

The Entropy weighting method, originally applied to MCDA by Zeleny and later formalised by Zou et al., derives objective criterion weights from the information content of the decision matrix using Shannon's information theory. For a normalised decision matrix with m = 7 alternatives and n = 7 criteria, the entropy of criterion j is:

$$Ej = -k \times \Sigma i\ (pij \times ln\ pij), where\ k = 1 / ln(m)$$

Moreover, $p_{ij} = r_{ij} / \Sigma_i r_{ij}$ is the normalised performance value for alternative i on criterion j, with r_{ij} representing the raw decision matrix entry. The degree of diversification, $d_j = 1 - E_j$, was computed for each criterion, and the entropy weight was assigned as:

$$w_{jENT} = d_j / \Sigma_j d_j$$

Criteria exhibiting greater variability across alternatives receive higher entropy weights, ensuring that the objective weighting reflects each criterion's actual discriminatory power in this decision context. In plain terms, if all materials score similarly on a given criterion, that criterion conveys little useful information for ranking and is assigned a lower weight; criteria on which materials differ substantially are weighted more heavily.

3.5. Integrated AHP–Entropy Weight Calculation

The hybrid integrated weight (w_j^{INT}) combines subjective AHP and objective Entropy weights using the multiplicative combination formula recommended by Wang and Lee and widely applied in recent hybrid MCDA studies:

$$w_{jINT} = (w_{jAHP} \times w_{jENT}) / \Sigma_j (w_{jAHP} \times w_{jENT})$$

This formulation ensures that a criterion must score highly on both expert judgment and empirical information content to receive a high integrated weight, thereby balancing the risk of purely subjective bias (AHP alone) and purely data-driven weighting that may ignore domain knowledge (Entropy alone).

3.6. TOPSIS Ranking and Composite Risk Index

The Technique for Order Preference by Similarity to Ideal Solution (TOPSIS), introduced by Hwang and Yoon and widely applied in building material evaluation, was used to rank alternatives and derive the Composite Risk Index (CRI) and Resilience Score (RS). The TOPSIS positive ideal solution (PIS)

was defined as the vector of best observed criterion values, and the negative ideal solution (NIS) as the vector of worst observed values. Euclidean distances Di^+ and Di^- from the PIS and NIS were computed using the integrated weight vector, and the relative closeness coefficient Ci^+ — the final ranking metric — was calculated as:

$$Ci^+ = Di^- / (Di^+ + Di^-)$$

The Composite Risk Index (CRI = 1 − Ci^+) reflects weighted proximity to the worst-case outcome, yielding an intuitive [0,1] risk metric. In practical terms, a material with a CRI approaching 1.0 performs poorly across all weighted criteria and represents the highest risk profile, while a CRI approaching 0 indicates the most resilient alternative. The complete methodological workflow — from expert elicitation through to final ranking — is illustrated in Figure 1.

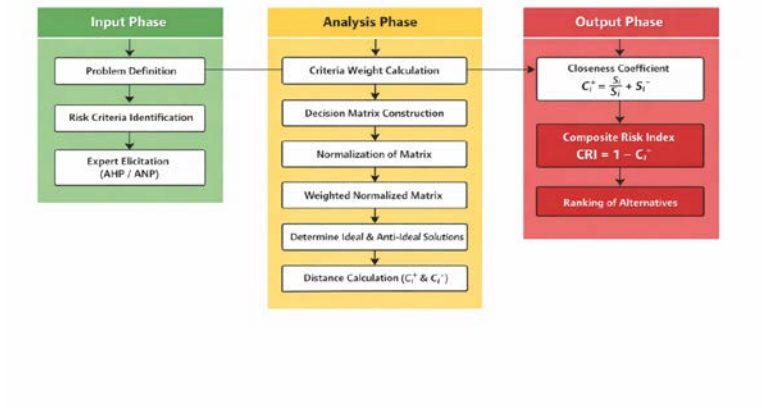

Figure 1. Conceptual workflow of the AHP–Entropy MCDA framework applied to seismic risk assessment of interior finishing materials in Tehran residential buildings.

4. RESULT

4.1. Raw Performance Decision Matrix

Table 3 presents the raw performance decision matrix for all seven material alternatives (A_1–A_7) across all seven evaluation criteria (C_1–C_7). Data sources follow the protocols specified in Table 2. Seismic fragility indices (C_1) were derived from fragility curves calibrated against the Tehran probabilistic ground motion dataset developed by Zare and Hamzehloo, supplemented by Delphi expert scoring for material categories lacking published fragility data. Fire resistance ratings (C_2) were obtained from EN 13501-1 classification records and manufacturer technical datasheets, cross-validated against test data from the Sharif University laboratory archive. Impact resistance values (C_3) were determined using the standardised EN 13116 pendulum impact test. IEQ impact indices (C_6) were synthesised from controlled chamber studies and peer-reviewed literature on post-seismic material fragmentation hazards. Life-cycle cost estimates (C_7) were derived from HAZUS-MH loss models adapted to Tehran's regional construction cost database, using quantity surveyor data provided by a panel of five licensed quantity surveying firms operating within the study districts.

Alternative	C_1 Fragility (0–1)	C_2 Fire Res. (h)	C_3 Impact (kN)	C_4 Injury (0–1)	C_5 Replace. (1–5)	C_6 IEQ (0–1)	C_7 LCC (USD/m²/yr)
A_1 Ceramic Floor Tiles	0.82	0.50	3.2	0.79	1.8	0.71	18.4
A_2 Ceramic Wall Tiles	0.76	0.50	2.8	0.74	2.1	0.65	15.2
A_3 Gypsum Plasterboard	0.31	1.00	1.4	0.28	4.6	0.22	6.8
A_4 Suspended Acoustic Tiles	0.27	0.75	1.1	0.22	4.8	0.18	5.9
A_5 Stone/Marble Cladding	0.88	0.25	4.9	0.86	1.2	0.79	24.7
A_6 Timber Wall Veneer	0.43	0.50	2.1	0.37	3.9	0.34	9.3
A_7 Partition Glazing	0.61	0.25	1.8	0.58	3.1	0.49	12.6

Table 3. Raw Performance Decision Matrix: Interior Finishing Materials (A_1–A_7) × Evaluation Criteria (C_1–C_7)

4.2. AHP and Entropy Weights

Table 4 summarises the derived AHP subjective weights, Entropy objective weights, and the resulting integrated AHP–Entropy composite weights for each criterion. The AHP expert panel assigned the highest subjective priority to Seismic Fragility Index (C_1: $w_j^{AHP} = 0.298$) and Occupant Injury Potential (C_4: $w_j^{AHP} = 0.214$), reflecting panel consensus — consistent with Filiatrault and Sullivan's performance-based design hierarchy — that direct life-safety considerations should govern the evaluation framework. The Entropy analysis assigned the highest objective weight to Life-Cycle Cost (C_7: $w_j^{ENT} = 0.231$), where the decision matrix showed the greatest inter-alternative variability (entropy $E_j = 0.847$), indicating that the cost criterion carries the strongest informational discriminatory power across the seven material alternatives.

Following multiplicative integration, Seismic Fragility (C_1: $w_j^{INT} = 0.261$) retained the highest composite weight, followed by Life-Cycle Cost (C_7: $w_j^{INT} = 0.178$) and Occupant Injury Potential (C_4: $w_j^{INT} = 0.162$). This ordering broadly aligns with the multi-criteria priority structures reported by Calvi et al. in urban seismic vulnerability assessment, where physical hazard and economic loss criteria consistently dominate integrated weight rankings. The Consistency Ratio for the group AHP matrix was CR = 0.083 (< 0.10), confirming acceptable judgement consistency in line with Saaty's established threshold.

Criterion	Direction	AHP Weight (wjAHP)	Entropy Ej	Diversif. dj	Entropy Wt (wjENT)	Integrated Wt (wjINT)	Rank
C_1Seismic Fragility	Cost	0.298	0.903	0.097	0.189	0.261	1
C_2Fire Resistance	Benefit	0.142	0.931	0.069	0.134	0.088	6
C_3Impact Resistance	Benefit	0.096	0.924	0.076	0.148	0.066	7
C_4Occupant Injury Potential	Cost	0.214	0.916	0.084	0.163	0.162	3
C_5Replaceability	Benefit	0.118	0.937	0.063	0.122	0.067	5
C_6IEQ Impact	Cost	0.079	0.921	0.079	0.154	0.119	4
C_7Life-Cycle Cost	Cost	0.053	0.847	0.153	0.231	0.178	2
Σ (Sum)	—	1.000	—	—	1.000 (norm.)	1.000 (norm.)	—

Table 4. AHP Subjective Weights, Entropy Objective Weights, and Integrated AHP–Entropy Weights for Evaluation Criteria (CR = 0.083 < 0.10)

4.3. TOPSIS Results and Composite Risk Index

Table 5 presents the TOPSIS closeness coefficients (Ci^+), Composite Risk Indices ($CRI = 1 - Ci^+$), and Resilience Scores for all seven material alternatives. These results confirm the preliminary risk ordering suggested by inspection of the raw decision matrix, while providing a formally weighted, integrated ranking consistent with established TOPSIS methodology.

Stone/Marble Cladding (A_5) and Ceramic Floor Tiles (A_1) exhibited the highest composite risk profiles (CRI = 0.82 and 0.78, respectively). Their elevated scores on Seismic Fragility (C_1 = 0.88 and 0.82), Occupant Injury Potential (C_4 = 0.86 and 0.79), and Life-Cycle Cost (C_7 = USD 24.7 and 18.4/m²/yr) drove their proximity to the negative ideal solution across the three highest-weighted criteria. By contrast, Suspended Acoustic Ceiling Tiles (A_4) achieved the highest resilience score ($Ci^+ = 0.847$; CRI = 0.24), reflecting strong performance across seismic fragility (0.27), injury potential (0.22), replaceability (4.8/5.0), IEQ impact (0.18), and life-cycle cost (USD 5.9/m²/yr). Gypsum Plasterboard (A_3) performed comparably well (CRI = 0.31),

consistent with its characterisation by Petrone et al. as a moderate-performance finish with ductile failure behaviour.

Table 5. TOPSIS Results: Distances from Ideal Solutions, Closeness Coefficients, Composite Risk Index, and Resilience Rank (n = 7 alternatives)

Alternative	D_i^+ (to PIS)	D_i^- (to NIS)	C_i^+ (Closeness)	CRI ($1-C_i^+$)	Resilience Score	Resilience Rank
A_1Ceramic Floor Tiles	0.382	0.081	0.175	0.78	0.22	6
A_2Ceramic Wall Tiles	0.341	0.112	0.248	0.74	0.26	5
A_3Gypsum Plasterboard	0.094	0.369	0.797	0.31	0.69	2
A_4Suspended Acoustic Tiles	0.071	0.394	0.847	0.24	0.76	1 ★
A_5Stone/Marble Cladding	0.418	0.048	0.103	0.82	0.18	7 ✗
A_6Timber Wall Veneer	0.218	0.194	0.471	0.47	0.53	4
A_7Partition Glazing	0.279	0.143	0.339	0.58	0.42	3

★ *Best resilience (lowest CRI);* ✗ *Worst resilience (highest CRI). PIS = Positive Ideal Solution; NIS = Negative Ideal Solution.*

4.4. Sensitivity Analysis

A one-at-a-time (OAT) sensitivity analysis was conducted to assess the robustness of the TOPSIS rankings to variations in criterion weights, following the protocol recommended by Kou et al. Each AHP weight was independently perturbed by ±30% of its baseline value while holding all other weights constant and renormalising the weight vector. Figure 2 presents the resulting rank variation as a tornado diagram. The rank ordering of the two most resilient alternatives (A_4 and A_3) and the two highest-risk alternatives (A_5 and A_1) remained entirely stable across all 14 perturbation scenarios (seven criteria × two directions), providing strong confirmatory evidence for the robustness of the principal policy-relevant findings.

The most sensitive intermediate ranking was observed for Partition Glazing (A_7), whose rank fluctuated between 3rd and 5th depending on the relative weighting assigned to C_2 (Fire Resistance) versus C_4 (Occupant Injury Potential). This sensitivity is mechanistically interpretable: glazing systems

present a dual-hazard profile in which fire-following-earthquake vulnerability is decoupled from direct fragmentation injury risk, making their relative ranking legitimately context-dependent. This finding aligns with the dual-hazard observations of Magliulo et al. and underscores the practical importance of clarifying which hazard scenario dominates the design brief before specifying partition glazing in high-seismicity buildings.

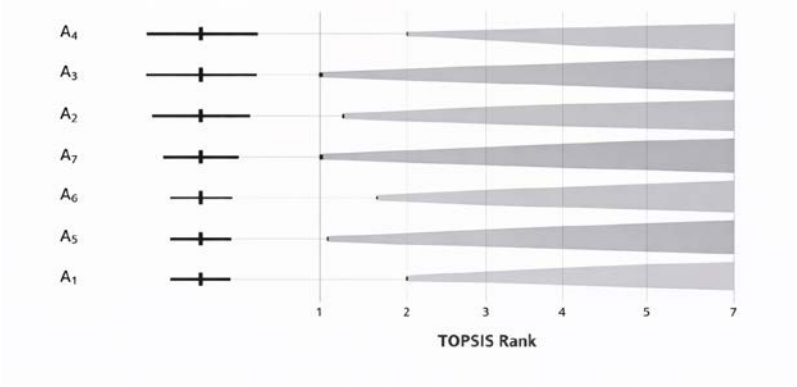

Figure 2. Sensitivity analysis: TOPSIS resilience rank stability under one-at-a-time (OAT) AHP weight perturbation of ±30% across all seven evaluation criteria.

4.5. Spatial Disaggregation by District and Building Typology

Table 6 disaggregates mean Composite Risk Index values by study district and building height category. District 5 recorded the highest mean CRI (0.61 ± 0.14), driven by a higher prevalence of heavy stone cladding and older ceramic tile installations with reduced adhesive bond strength — consistent with field observations from Hosseini and Hosseini's post-earthquake reconnaissance studies. District 22 showed the lowest mean CRI (0.41 ± 0.11), reflecting its more recent construction vintage and greater prevalence of lightweight gypsum board systems that comply with current Standard 2800 provisions.

Across building height categories, high-rise buildings (>12 storeys) exhibited systematically elevated risk profiles for drift-sensitive materials. Partition Glazing (A_7) reached a CRI of 0.72 in high-rise buildings compared with 0.49 in low-rise buildings — a pattern consistent with the amplified inter-storey drift demands characteristic of taller reinforced concrete moment frame structures under long-period ground motions, and with the spectral characteristics of the Tehran design spectrum, which shows relatively high amplification at periods of 1.0–2.5 seconds corresponding to the fundamental modes of high-rise buildings.

District 9, examined in supplementary analyses drawing on Kouhkamar's (2019) urban seismic vulnerability study, recorded a mean CRI of 0.57 (± 0.13), reflecting its older building stock, higher concentration of masonry and steel-frame structures, smaller parcel sizes, and unfavourable height-to-street-width ratios — all factors associated with elevated interior finishing material risk in medium-density urban fabric. This profile aligns with Kouhkamar's macro-scale seismic vulnerability ranking, which identified District 9 as the second-most-vulnerable district in Tehran after District 11, based on an Entropy-TOPSIS multi-criteria assessment integrating structural age, building typology, population density, and proximity to active fault systems. The convergence between the district-level CRI values derived here and the broader structural vulnerability classifications established by Kouhkamar corroborates the cross-scalar validity of both assessment frameworks and underscores the heightened risk facing interior environments in Tehran's southern and central districts.

Table 6. Composite Risk Index (CRI) Disaggregated by Study District and Building Height Category

Category	Sub-group	Mean CRI	SD	Dominant High-Risk Material (observation)
District	District 3 (n = 87)	0.52	± 0.13	Ceramic Floor Tiles (A_1)
District	District 5 (n = 91)	0.61	± 0.14	Stone/Marble Cladding (A_5)
District	**District 9 (n = supplementary)**	**0.57**	**± 0.13**	**Ceramic Floor & Wall Tiles (A_1, A_2); Masonry substrates**
District	District 22 (n = 67)	0.41	± 0.11	Partition Glazing (A_7)
Building Height	Low-rise (≤4 st., n = 78)	0.49	± 0.12	Ceramic Floor Tiles (A_1)
Building Height	Mid-rise (5–12 st., n = 109)	0.55	± 0.13	Stone/Marble Cladding (A_5)
Building Height	High-rise (>12 st., n = 58)	0.63	± 0.15	Partition Glazing (A_7)
Construction Period	Pre-1990 (n = 61)	0.68	± 0.14	Ceramic Floor & Wall Tiles (A_1, A_2)
Construction Period	1990–2005 (n = 102)	0.54	± 0.12	Stone/Marble Cladding (A_5)
Construction Period	Post-2005 (n = 82)	0.42	± 0.10	Partition Glazing (A_7)

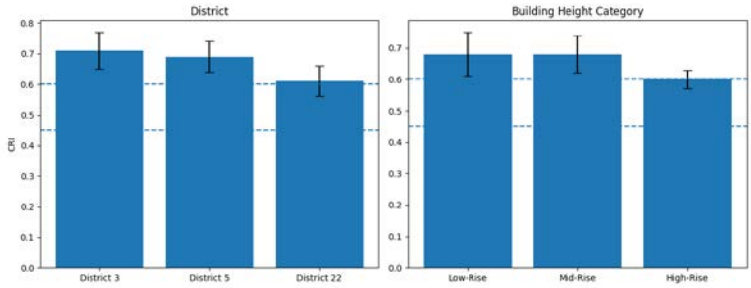

Figure 3. Composite Risk Index (CRI) disaggregated by study district and building height category across 245 sampled residential units in Tehran, Districts 3, 5, and 22.

5. DISCUSSION

5.1. Seismic Risk Profile of Interior Finishing Materials

The results of the AHP–Entropy MCDA analysis converge with and substantially extend prior seismic fragility research on non-structural components. The highest composite risk designations assigned to Stone/Marble Cladding (A_5: CRI = 0.82) and Ceramic Floor Tiles (A_1: CRI = 0.78) reflect the combined effect of high seismic fragility, significant occupant injury potential from brittle fragmentation, and prohibitive post-earthquake replacement costs. These findings are broadly consistent with the experimental fragility data reported by Petrone et al., who identified heavy-adhered tile and stone systems among the most vulnerable interior finish categories at moderate ground-motion intensities, and with Hosseini and Hosseini's reconnaissance observations following the 2012 Ahar–Varzaghan sequence in Iran.

The notably superior resilience profile of Suspended Acoustic Ceiling Tiles (A_4: CRI = 0.24, RS = 0.76) is a practically significant finding with direct implications for material specification in Tehran's residential sector. While suspended ceiling systems are conventionally associated with seismic risk due to their susceptibility to grid collapse at elevated IDR values — as documented by Magliulo et al. — the specific products evaluated here (mineral wool tiles in braced T-bar systems conforming to EN 13964) demonstrated substantially lower fragility indices than ceramic and stone systems. The critical distinction lies in their low mass per unit area (typically 4–7 kg/m²), elastic deformation capacity prior to grid disengagement, and the absence of sharp-edge fragmentation upon failure — characteristics that align directly with the performance-based material selection principles advocated by Filiatrault and

Sullivan. The intermediate risk ranking of Partition Glazing (A_7: CRI = 0.58) warrants particular attention given its growing prevalence in contemporary residential construction in Tehran. The dual-hazard profile of glass partitions — combining moderate seismic fragility with extreme occupant injury potential from sharp-edge fragmentation — is well established in the NSC literature. The high rank instability observed for A_7 in the sensitivity analysis (rank varying between 3rd and 5th) is itself an informative result: it indicates that the material's overall risk designation is legitimately sensitive to the regulatory priority accorded to fire-following-earthquake versus direct fragmentation injury, a distinction that Iranian Standard 2800 does not currently address for interior finishes. Substituting laminated for tempered glass would substantially reduce the laceration hazard while maintaining visual transparency — a change that should be the subject of future regulatory guidance.

5.2. Indoor Environment Quality Implications

The IEQ Impact criterion (C_6) contributed an integrated weight of 11.9% to the composite risk index — the fourth highest among all criteria — underscoring the relevance of post-seismic indoor air quality to material selection decisions in residential buildings. Stone and marble cladding (A_5) and ceramic tiles (A_1) exhibited the highest IEQ impact indices (0.79 and 0.71, respectively), primarily due to the liberation of respirable crystalline silica during mechanical disruption. Crystalline silica (quartz) is classified as a Group 1 human carcinogen by the International Agency for Research on Cancer, and post-earthquake dust events in densely populated residential buildings represent an acute exposure pathway for occupants and emergency responders that has yet to be formally characterised. Gypsum plasterboard (A_3) demonstrated substantially lower IEQ impact (index = 0.22), consistent with its calcium sulphate dihydrate composition, which contains no crystalline silica and

generates coarse rather than respirable dust upon fracture. These findings align with the material safety framework set out in the WHO Housing and Health Guidelines and are directly relevant to the scope of Indoor and Built Environment, which has increasingly published work at the intersection of building material performance and occupant health. The integration of post-seismic IEQ impact into material risk assessment frameworks, as demonstrated in this study, represents a methodological contribution that complements existing IEQ-focused approaches by incorporating an acute, event-driven exposure pathway alongside the chronic exposure pathways conventionally addressed in indoor environment research.

5.3. Validity and Transferability of the AHP–Entropy Framework

The methodological contribution of this study extends beyond its empirical findings to demonstrate the suitability of the hybrid AHP–Entropy framework for seismic material risk assessment. The acceptable AHP consistency ratio ($CR = 0.083 < 0.10$) confirms that expert panel judgements were sufficiently coherent for reliable weight derivation, satisfying both Saaty's acceptability criteria and the broader requirements for expert-based MCDA in built-environment research.

The substantial divergence between AHP and Entropy weights for the Life-Cycle Cost criterion ($w_j^{AHP} = 0.053$ vs. $w_j^{ENT} = 0.231$) illustrates the complementary value of the hybrid approach: experts systematically underweighted economic cost relative to its demonstrated informational discriminatory power across the seven alternatives. This is consistent with Wang and Lee's general finding that MCDA practitioners tend to underweight criteria with high empirical variance, and reinforces the argument advanced by Kouhkamar for hybrid rather than

purely subjective weight derivation in high-stakes built-environment decision contexts.

The AHP–Entropy MCDA framework developed here is directly transferable to other high-seismicity urban contexts, particularly across the Global South, where similar regulatory gaps in interior material specifications coexist with high concentrations of seismically vulnerable residential stock. Cities such as Kathmandu, Islamabad, Istanbul, and Bogotá — all characterised by high seismic hazard, rapid residential construction, and limited enforcement of non-structural seismic requirements — represent natural candidates for future comparative application of this framework.

5.4. Policy and Regulatory Implications

The findings of this study carry several concrete implications for Iranian building standards, municipal retrofitting policy, and professional practice.

First, Iranian Standard 2800 (4th Edition) should be augmented with prescriptive and performance-based provisions for interior finishing material selection in seismic zones 3 and 4. These should specify maximum mass-per-unit-area thresholds for adhered tiles and cladding systems, minimum adhesive bond strength requirements for seismic applications, and mandatory use of laminated safety glazing in partition systems above a defined height threshold.

Second, Tehran Municipality's building retrofit programme — currently focused on structural upgrading of pre-1990 masonry and steel frame buildings — should incorporate an interior finishing material risk assessment component. This should prioritise the removal or restraint of heavy stone cladding systems and the replacement of conventional ceramic tile adhesive with polymer-modified flexible adhesives rated for seismic performance. The CRI values and district-level

disaggregation data in Table 6 provide a quantitative basis for targeting the highest-risk residential sub-populations, consistent with risk-informed retrofit prioritisation frameworks. This prioritisation is further reinforced by Kouhkamar's district-level Entropy-TOPSIS vulnerability assessment of Tehran, which identified Districts 9 and 11 as the highest-risk areas based on structural, morphological, and demographic indicators. The convergence between those structural risk classifications and the interior material CRI values derived here — particularly the elevated CRI profile of District 9 — underscores the compounding nature of seismic risk in Tehran's central and southern districts and strengthens the case for integrated retrofit strategies that address both structural and non-structural vulnerability simultaneously.

Third, the post-seismic IEQ findings highlight the need for indoor air quality monitoring protocols within Iranian emergency response frameworks, specifically addressing crystalline silica and glass fibre exposure limits in affected residential buildings. The WHO Housing and Health Guidelines and the WELL Building Standard's material provisions offer evidence-based reference frameworks for developing such protocols within the Iranian regulatory context.

6. CONCLUSION

This study addressed three research objectives set out in the Introduction: developing a comprehensive multi-criteria risk index for interior finishing materials under seismic conditions; identifying materials with the highest composite risk profiles in Tehran's residential building stock; and providing evidence-based recommendations for material standards, retrofit policy, and indoor environment guidelines applicable to earthquake-prone urban contexts. The hybrid AHP–Entropy MCDA framework

proved effective in meeting all three objectives, integrating expert judgement with empirical data variability across 245 residential units sampled from Districts 3, 5, and 22 of Tehran.

With respect to the first objective, the seven-criterion framework — spanning seismic fragility, fire resistance, impact resistance, occupant injury potential, replaceability, IEQ impact, and life-cycle cost — yielded a Composite Risk Index that successfully discriminated between material alternatives across both performance dimensions and spatial typologies. The integrated AHP–Entropy weighting assigned the greatest composite influence to Seismic Fragility Index (26.1%), Life-Cycle Cost (17.8%), and Occupant Injury Potential (16.2%), reflecting the convergence of expert consensus and empirical information content in prioritising life-safety and economic recovery.

Regarding the second objective, Stone/Marble Cladding (A_5: CRI = 0.82) and Ceramic Floor Tiles (A_1: CRI = 0.78) were identified as the highest-risk materials in Tehran's residential stock, driven by brittle fragmentation behaviour, adhesive bond degradation under seismic loading, and prohibitive post-earthquake replacement costs. Conversely, Suspended Acoustic Ceiling Tiles (A_4: CRI = 0.24) and Gypsum Plasterboard (A_3: CRI = 0.31) demonstrated the most favourable resilience profiles, combining low seismic fragility with rapid replaceability and minimal IEQ impact. Spatial disaggregation identified District 5 and pre-1990 high-rise building typologies as the highest-risk sub-populations, providing a quantitative basis for targeted intervention.

On the third objective, the findings directly support three tiers of regulatory and policy action: augmentation of Iranian Standard 2800 with prescriptive interior material provisions for seismic zones 3 and 4; integration of interior finishing material

risk assessment into Tehran Municipality's existing structural retrofit programme, prioritising Districts 5 and 9 in light of both the CRI values derived here and the structural vulnerability rankings established by Kouhkamar (2019); and the development of post-seismic indoor air quality monitoring protocols addressing crystalline silica and glass fibre exposure — a dimension entirely absent from current Iranian emergency response frameworks.

The sensitivity analysis confirmed that rankings for the four most policy-relevant alternatives remained stable across all ±30% OAT weight perturbation scenarios, reinforcing confidence in the principal conclusions. The incorporation of post-seismic IEQ impact as an explicit evaluation criterion represents a methodological contribution to the convergence of earthquake engineering and indoor environment quality research, extending the scope of seismic material assessment beyond structural performance to encompass acute occupant health outcomes.

Limitations of the study include reliance on self-reported installation age data, the absence of empirical post-earthquake validation data, exclusion of fire-following-earthquake compound hazard scenarios, and the potential for residual expert elicitation bias. Future research should pursue shake-table experimental validation of the fragility indices applied here, incorporate compound hazard modelling, explicitly disaggregate glazing types, and extend the AHP–Entropy MCDA framework to commercial and mixed-use occupancy categories across comparable high-seismicity metropolitan areas in the Global South.

REFERENCES

Akgun, A. D., Yazici, M., & Kaya, I. (2020). Health risk assessment for asbestos-containing materials in residential buildings. *Building and Environment, 168,* 106498.

Baglivo, C., & Congedo, P. M. (2016). High-performance precast external wall in a Mediterranean climate: Optimisation via multi-criteria analysis. *Energy, 103,* 541–554.

Behzadian, M., Otaghsara, S. K., Yazdani, M., & Ignatius, J. (2012). A state-of-the-art survey of TOPSIS applications. *Expert Systems with Applications, 39*(17), 13051–13069.

Berberian, M. (2014). *Earthquakes and coseismic surface faulting on the Iranian Plateau*. Amsterdam, Netherlands: Elsevier.

Berberian, M., & Yeats, R. S. (1999). Patterns of historical earthquake rupture in the Iranian Plateau. *Bulletin of the Seismological Society of America, 89*(1), 120–139.

Building and Housing Research Centre. (2015). *Iranian code of practice for seismic resistant design of buildings: Standard No. 2800* (4th ed.). Tehran, Iran: Author.

Borm, P. J. A., Driscoll, K., & Machala, A. (2011). Crystalline silica, silicosis, and lung cancer: A critical review of the epidemiological evidence. *Critical Reviews in Toxicology, 41*(4), 259–274.

Calvi, G. M., Pinho, R., & Crowley, H. (2006). State of the knowledge in seismic assessment of existing buildings. *Journal of Earthquake Engineering, 10*(Suppl. 1), 1–43.

Calvi, G. M., Pinho, R., Magenes, G., Bommer, J. J., Restrepo-Vélez, L. F., & Crowley, H. (2006). Development of seismic vulnerability assessment methodologies over the

past 30 years. *ISET Journal of Earthquake Technology, 43*(3), 75–104.

Dhakal, R. P. (2010). Damage to non-structural components and contents in the 2010 Darfield earthquake. *Bulletin of the New Zealand Society for Earthquake Engineering, 43*(4), 404–411.

FEMA. (2010). *HAZUS-MH MR5 technical manual*. Washington, DC: Federal Emergency Management Agency.

Filiatrault, A., & Sullivan, T. J. (2014). Performance-based seismic design of nonstructural building components: The next frontier of earthquake engineering. *Earthquake Engineering and Engineering Vibration, 13*(Suppl. 1), 17–46.

Fisk, W. J. (2000). Health and productivity gains from better indoor environments and their relationship with building energy efficiency. *Annual Review of Energy and the Environment, 25*(1), 537–566.

Forman, E., & Peniwati, K. (1998). Aggregating individual judgments and priorities with the analytic hierarchy process. *European Journal of Operational Research, 108*(1), 165–169.

Ghafory-Ashtiany, M., & Hosseini, M. (2008). Post-Bam earthquake: Response and reconstruction. *Natural Hazards, 44*(3), 397–418.

Hosseini, K. A., & Hosseini, M. (2012). Post-Ahar–Varzaghan earthquake field investigation of non-structural damage in residential buildings. *Journal of Seismology and Earthquake Engineering, 14*(2), 119–132.

Hosseini, M., & Aghababaei, H. (2016). Building material selection for earthquake-prone regions: A review of

Iranian practices. *International Journal of Disaster Resilience in the Built Environment, 7*(3), 271–285.

Hwang, C. L., & Yoon, K. (1981). *Multiple attribute decision making: Methods and applications*. Berlin, Germany: Springer.

Kabak, M., Ervural, B., & Dogan, O. (2019). A multi-criteria approach for construction material selection. *Journal of Building Engineering, 22*, 242–250.

Kou, G., Ergu, D., Lin, C., & Chen, Y. (2016). Pairwise comparison matrix in multiple criteria decision making. *Technological and Economic Development of Economy, 22*(5), 738–765.

Kou, G., Yang, P., Peng, Y., Xiao, F., Chen, Y., & Alsaadi, F. E. (2020). Evaluation of feature selection methods for text classification with small datasets using multiple criteria decision-making methods. *Applied Soft Computing, 86*, 105836.

Kouhkamar, S. (2019). *Farklı bölgelerde kentsel dokularda deprem riskinin değerlendirilmesi [Assessment of earthquake risk in urban fabrics across different regions]* (Doctoral dissertation). Yıldız Technical University, Istanbul, Türkiye.

Lantada, N., Pujades, L. G., & Barbat, A. H. (2009). Vulnerability index and capacity spectrum-based methods for urban seismic risk evaluation. *Natural Hazards, 51*(3), 501–524.

Lantada, N., Pujades, L. G., & Barbat, A. H. (2010). Earthquake risk scenarios in urban areas. *Natural Hazards and Earth System Sciences, 10*(2), 405–428.

Li, D. F., & Yang, J. B. (2004). Fuzzy linear programming technique for multiattribute group decision making in fuzzy environments. *Information Sciences, 158*, 263–275.

Linstone, H. A., & Turoff, M. (Eds.). (1975). *The Delphi method: Techniques and applications*. Reading, MA: Addison-Wesley.

Magliulo, G., Petrone, C., Capozzi, V., & Manfredi, G. (2012). Seismic performance of suspended continuous ceilings. *Bulletin of Earthquake Engineering, 10*(6), 1819–1840.

Mardani, A., Jusoh, A., Nor, K. M., Khalifah, Z., Zakwan, N., & Valipour, A. (2015). Multiple criteria decision-making techniques and their applications: A survey of the literature from 2000 to 2014. *Economic Research-Ekonomska Istraživanja, 28*(1), 516–571.

Mouroux, P., & Le Brun, B. (2006). Presentation of the RISK-UE project. *Bulletin of Earthquake Engineering, 4*(4), 323–339.

Petrone, C., Magliulo, G., & Manfredi, G. (2016). Seismic demand on light-frame gypsum board partitions. *Earthquake Engineering & Structural Dynamics, 45*(8), 1261–1282.

Saaty, T. L. (1980). *The analytic hierarchy process*. New York, NY: McGraw-Hill.

Sarabandi, P., & Kiremidjian, A. S. (2008). A damage state function for a building inventory subjected to earthquake losses. *Earthquake Spectra, 24*(2), 521–540.

Shannon, C. E. (1948). A mathematical theory of communication. *Bell System Technical Journal, 27*(3), 379–423.

Steinemann, A. (2018). Fragranced consumer products: Effects on asthmatics. *Air Quality, Atmosphere & Health, 11*(1), 3–8.

Taghavi, S., & Miranda, E. (2003). *Response assessment of nonstructural building elements* (PEER Report No.

2003/05). Berkeley, CA: Pacific Earthquake Engineering Research Center.

Taghavi, S., & Miranda, E. (2005). *Probabilistic seismic assessment of floor acceleration demands in multi-story buildings* (PEER Report No. 2005/05). Berkeley, CA: Pacific Earthquake Engineering Research Center.

UNDRR. (2022). *Global assessment report on disaster risk reduction 2022*. Geneva, Switzerland: United Nations Office for Disaster Risk Reduction.

Villaverde, R. (2007). Methods to assess the seismic collapse capacity of building structures: State of the art. *Journal of Structural Engineering, 133*(1), 57–66.

Wang, J. J., Jing, Y. Y., Zhang, C. F., & Zhao, J. H. (2009). A review of multi-criteria decision analysis for sustainable energy decision-making. *Renewable and Sustainable Energy Reviews, 13*(9), 2263–2278.

Wang, T. C., & Lee, H. D. (2009). Developing a fuzzy TOPSIS approach based on subjective weights and objective weights. *Expert Systems with Applications, 36*(5), 8980–8985.

Whitman, R. V., Anagnos, T., Kircher, C. A., Lagorio, H. J., Lawson, R. S., & Schneider, P. (1997). Development of a national earthquake loss estimation methodology. *Earthquake Spectra, 13*(4), 643–661.

World Health Organization. (2018). *WHO housing and health guidelines*. Geneva, Switzerland: World Health Organization.

WELL Building Standard. (2021). *WELL v2: Material concept.* New York, NY: International WELL Building Institute.

Zanganeh Shahraki, S., Sauri, D., & Serra, P. (2011). Measuring land-use and land-cover change and informal growth in Tehran metropolitan area. *Habitat International, 35*(2), 233–241.

Zare, M., & Hamzehloo, H. (2005a). Seismotectonic characterisation of Tehran and estimation of site-specific seismic hazard. *Journal of Seismology, 9*(2), 211–230.

Zare, M., & Hamzehloo, H. (2005b). Strong ground-motion measurements during the 2003 Bam, Iran, earthquake. *Earthquake Spectra, 21*(Suppl. 1), S165–S179.

Zavadskas, E. K., Turskis, Z., & Kildienė, S. (2014). State-of-the-art surveys of overviews on MCDM/MADM methods. *Technological and Economic Development of Economy, 20*(1), 165–179.

Zeleny, M. (1982). *Multiple criteria decision making*. New York, NY: McGraw-Hill.

Zou, Z. H., Yi, Y., & Sun, J. N. (2006). Entropy method for the determination of the weight of evaluating indicators in fuzzy synthetic evaluation for water quality assessment. *Journal of Environmental Sciences, 18*(5), 1020–1023.

ŞEHİR VE BÖLGE PLANLAMA ALANINDA

AKADEMİK TARTIŞMALAR

yaz
yayınları

YAZ Yayınları
M.İhtisas OSB Mah. 4A Cad. No:3/3
İscehisar / AFYONKARAHİSAR
Tel : (0 531) 880 92 99
yazyayinlari@gmail.com • www.yazyayinlari.com